PAPER

NJC
www.rsc.org/njc

Distance-independent photoinduced energy transfer over 1.1 to 2.3 nm in ruthenium trisbipyridine–fullerene assemblies†

Frédérique Chaignon,[a] Javier Torroba,[a] Errol Blart,[a] Magnus Borgström,[b] Leif Hammarström*[b] and Fabrice Odobel*[a]

[a] *Laboratoire de Synthèse Organique, UMR 6513 CNRS, Faculté des Sciences et des Techniques de Nantes, BP 92208, 2, rue de la Houssinière, 44322 Nantes Cedex 03, France. E-mail: Fabrice.Odobel@chimie.univ-nantes.fr; Fax: +33 2 51 12 54 02; Tel: +33 2 51 12 54 29*

[b] *Department of Physical Chemistry, Uppsala University, Box 579, SE-751 23 Uppsala, Sweden. E-mail: Leifh@fki.uu.se; Fax: +46 18 471 3654*

Received (in Montpellier, France) 16th May 2005, Accepted 26th July 2005
First published as an Advance Article on the web 26th August 2005

Ruthenium trisbipyridine C_{60} dyads linked *via para*-phenyleneethynylene units have been prepared. They displayed a rapid energy transfer from Ru to C_{60} with a rate that was independent of distance, from 1.1 to 2.3 nm. The results are explained by a hopping mechanism involving a bridge-localized excited-state. In fact, for the longest bridge this state was lower in energy than the Ru-based MLCT state, as evidenced by the spectroscopic data.

Introduction

There is a strong current interest in the preparation and study of molecular assemblies performing efficient long-range electron- or energy-transfer, mediated *via* an intervening bridge that links the reactant chromophoric and/or redox units together.[1] If the excited states or charge transfer states involving the bridge are not much higher in energy than the reactant state, the electron- or energy-transfer may proceed *via* a transient population of these bridge states.[2]

This mechanism is frequently referred to as ''hopping'', and as the resulting transfer process can be very efficient over long distances the molecular structure is often called a molecular electronic or photonic wire.[3]

In the present paper, we present a series of complexes based on a Ru^{II}–polypyridine chromophore and a fullerene acceptor, linked *via* a highly conjugated phenyl-ethynyl bridge of varying length (1.1–2.3 nm center to center distance was estimated from X-ray crystallographic data on similar building blocks from refs 4 and 5). This chromophore–acceptor couple has been employed in studies of electron- and energy-transfer.[6–8] The phenyl-ethynyl bridge motif has previously been shown to mediate rapid intra-molecular electron transfer.[9–13] The alkoxy substituents on the phenyl groups of the present study make electron transfer *via* reduced states of the bridge more difficult. Instead, they lower the excited state energy of the bridge and facilitate triplet energy transfer *via* a hopping mechanism.[4] We present the synthesis and triplet energy transfer properties of these complexes (Scheme 1).

Experimental

General methods

^{1}H and ^{13}C NMR spectra were recorded on a Bruker ARX 300 MHz or AMX 400 MHz Bruker spectrometer. Chemical shifts for ^{1}H NMR spectra are referenced relative to residual protium in the deuterated solvent ($CDCl_3$ δ = 7.26 ppm, MeOD δ = 3.31 ppm). Mass spectra were recorded on a EI-MS HP 5989A spectrometer or on a JMS-700 (JEOL LTD, Akishima, Tokyo, Japan) double focusing mass spectrometer of reversed geometry equipped with electrospray ionization (ESI) source. Fast atom bombardment mass spectroscopy (FAB-MS) analyses were performed in *m*-nitrobenzyl alcohol matrix (MBA) on a ZAB-HF-FAB spectrometer. MALDI-TOF analyses were performed on an Applied Biosystems Voyager DE-STR spectrometer in positive linear mode at 20 kV acceleration voltage with α-cyano 4-hydroxycinnamic acid (CHCA) as matrix.

Thin-layer chromatography (TLC) was performed on aluminium sheets precoated with Merck 5735 Kieselgel $60F_{254}$. Column chromatography was carried out either with Merck 5735 Kieselgel 60F (0.040–0.063 mm mesh) or with SDS neutral alumina (0.05–0.2 mm mesh). Air sensitive reactions were carried out under argon in dry solvents and glassware.

Chemicals were purchased from Aldrich and used as received. Compounds 4-trimethylsilylethynylbenzaldehyde, 5-bromobipyridine,[14] bischloro bisbipyridine ruthenium(II),[15] bischloro(diphenylphosphino) ferrocene palladium(II)[16] and tetrakis(triphenylphosphine) palladium[17] were prepared according to literature methods.

Electrochemistry

The electrochemical measurements were performed with a potentiostat–galvanostat MacLab model ML160 controlled by resident software (Echem v1.5.2 for Windows) using a conventional single-compartment three-electrode cell. The working electrode was a Pt wire of 10 mm long, the auxiliary was a Pt wire and the reference electrode was the saturated potassium chloride calomel electrode (SCE). The supported electrolyte was 0.15 N Bu_4NPF_6 in dichloromethane and the solutions were purged with argon before the measurements. All potentials are quoted relative to SCE. In all the experiments the scan rate was 100 mV s^{-1} for cyclic voltammetry and 15 Hz for pulse voltammetry.

† Electronic supplementary information (ESI) available: Transient absorption spectra and traces for $\mathbf{D_1}$–$\mathbf{D_3}$ and $\mathbf{R_1}$, and a Table with kinetic data from a global fit. See http://dx.doi.org/10.1039/b506837a

DOI: 10.1039/b506837a

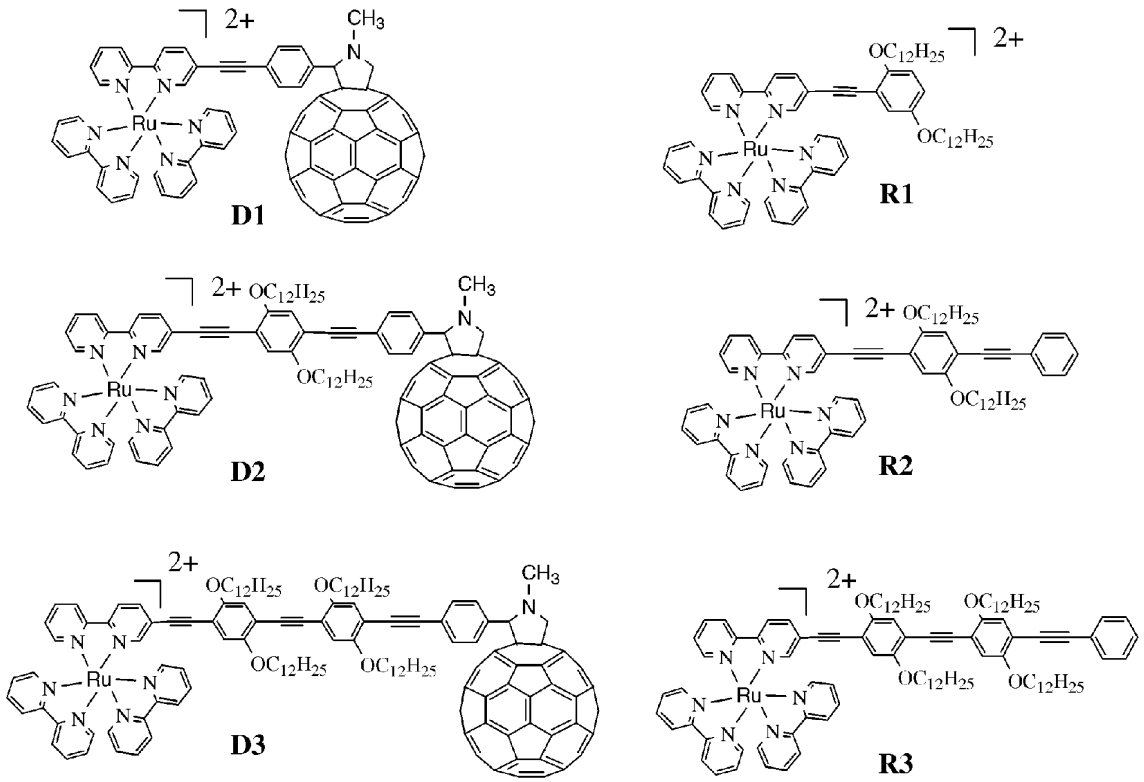

Scheme 1 Structures of the compounds studied in this work.

Spectroscopy

UV–Visible absorption spectra were recorded on a UV-2401PC Shimadzu spectrophotometer. Fluorescence spectra were recorded on a SPEX Fluoromax fluorimeter and were corrected for the wavelength dependent response of the detector system.

Time-resolved correlated single photon measurements were performed on a previously described system.[18] The emission was collected at magic angle polarization (55.4°) relative to the excitation light and the instrument had an response function with a FWHM of ~60 ps. Time-resolved emission and transient absorption data on the μs timescale were collected with a frequency tripled Q-switched Nd:YAG laser from Quantel. The output light was manipulated in an optical parametric oscillator (OPO) delivering <10 ns flashes at 460 nm with an energy ~15 mJ. The concentration of the samples in the emission experiments was controlled so the absorption at the pump wavelength was held around 0.1.

The laser pulses generated for the transient absorption pump–probe experiments have been previously described.[19] The 800 nm output was converted to 485 nm in an optical parametric amplifier (TOPAS). A mechanical chopper blocked every second pump beam and the energy of the beam was set below 2 μJ. The probe light was passed through a movable delay line allowing for a delay between pump and probe up to 10 ns. A vertically moving CaF_2 crystal in the probe beam produced a continuous white light and a $\lambda/2$-plate adjusted the polarization of the light so that the difference in polarization between pump and probe was fixed at magic angle conditions. The pump and probe beam were then focused in a vertically moving 1 × 10 mm cell. The transmitted probe light was divided spatially on an optical diffraction grating and further detected on a diode array. To adjust for differences in laser intensity part of the probe light was passed to the detector without passing the sample and the transient absorption was calculated as:

$$\Delta abs = -\log [(I_{probe,\tau=t}/I_{reference,\tau=t})/(I_{probe,\tau=0}/I_{reference,\tau=0})].$$

The reported values are averages of 5000–10 000 individual measurements. All optical experiments were performed in acetonitrile at 298 K.

Syntheses of the compounds

2,5-Bis(dodecyloxy)bromobenzene 2. Bromohydroquinone **1** (5 g, 26 mmol) was dissolved in DMF (25 mL). NaOH (2.6 g, 66 mmol) and 1-bromododecane (14.1 mL, 57 mmol) were added and the resulting solution was stirred at reflux for two days. Water (100 mL) was added and the solution was extracted with dichloromethane. The organic layer was washed with a saturated aqueous solution of NH_4Cl, dried over $MgSO_4$ and evaporated. The crude product was purified by flash chromatography (SiO_2, petroleum ether 100%, then petroleum ether–dichloromethane 95 : 5). Compound **2** was obtained as a white solid (8.5 g, 62%).

^{1}H NMR (300 MHz, $CDCl_3$): δ = 7.10 (d, J = 2.4 Hz, 1H), 6.81 (s, 1H), 6.79 (d, J = 2.4 Hz, 1H), 3.94 (t, J = 6.4 Hz, 2H), 3.87 (t, J = 6.4 Hz, 2H), 1.77 (m, 4H), 1.26 (m, 36H), 0.88 (m, 6H). ^{13}C NMR (300 MHz, $CDCl_3$): δ = 153.54, 149.73, 119.43, 114.65, 114.34, 112.74, 70.18, 68.79, 31.93, 29.66, 29.60, 29.37, 29.27, 26.00, 22.71, 14.14. EI-MS: $M^{+\bullet}$: 524.50 (37%), 356.20 (21%), 187.95 (87%), 110.10 (11%), 43.15 (100%). Mp: 49 °C.

2,5-Bis(dodecyloxy)-4-bromo-1-nitrobenzene 3. Compound **2** (4 g, 7.6 mmol) was dissolved in chloroform (12 mL) and acetic acid (13 mL) then the solution was stirred at room temperature for 10 min. The solution was cooled to 5 °C and a mixture of acetic acid (3.6 mL) and HNO_3 (1.6 mL, 34 mmol) was added dropwise for a whole hour. Chloroform (8 mL) was further added and the solution was stirred at room temperature for 18 h. Water (100 mL) was added and this solution was extracted with dichloromethane. The organic layer was dried over $MgSO_4$ and evaporated to yield **3** as a yellow solid (4.2 g, 97%).

^{1}H NMR (300 MHz, $CDCl_3$): δ = 7.41 (s, 1H), 7.30 (s, 1H), 4.02 (m, 4H), 1.81 (m, 4H), 1.26 (m, 36H), 0.88 (m, 6H).

^{13}C NMR (300 MHz, $CDCl_3$): δ = 153.56, 149.75, 119.45, 114.69, 114.38, 112.76, 70.22, 68.82, 31.93, 29.65, 29.37, 29.27, 26.00, 22.70, 14.14. EI-MS: $M^{+\bullet}$: 569.15 (3%), 400.95 (6%), 232.85 (100%). Mp: 63 °C.

2,5-Bis(dodecyloxy)-4-bromo-1-aminobenzene 4. Compound **3** (3.8 g, 6.6 mmol) was dissolved in THF (30 mL) and HCl (8 mL) was added. Tin powder (4 g, 34 mmol) was divided into 8 fractions that were slowly added. Then THF (20 mL) was added and the solution was stirred at room temperature for 18 h. The mixture was diluted with water (40 mL) and dichloromethane (80 mL) and K_2CO_3 were added to bring the pH of the solution to neutrality. The solution was filtered, the organic layer separated and rotary evaporated. The residue was dissolved in dichloromethane and the solution was washed with a saturated aqueous NaCl solution. The organic layer was dried over $MgSO_4$ and evaporated. Compound **4** was obtained as a beige solid (3.3 g, 92%).

^{1}H NMR (300 MHz, $CDCl_3$): δ = 6.91 (s, 1H), 6.37 (s, 1H), 3.91 (t, 4H), 3.80 (s, 2H); 1.77 (m, 4H), 1.26 (m, 36H), 0.88 (m, 6H). ^{13}C NMR (300 MHz, $CDCl_3$): δ = 149.94, 141.34, 137.37, 116.61, 102.70, 98.88, 70.22, 69.28, 31.93, 29.62, 29.37, 26.00, 22.70, 14.14. EI-MS: $M^{+\bullet}$: 541.50 (68%), 461.50 (32%), 292.30 (9%), 124.10 (29%) 43.15 (100%). Mp: 74 °C.

2,5-Bis(dodecyloxy)-4-bromo-(3′,3′-diethyltriazeno)benzene 5. Compound **4** (1.2 g, 2.2 mmol) was dissolved in THF (25 mL) under nitrogen. The solution was degassed and cooled to −8 °C. $BF_3 \cdot Et_2O$ (0.42 mL, 3.3 mmol) diluted with THF (0.6 mL) and was injected. After 10 min, $tBuNO_2$ (0.32 mL, 2.7 mmol) diluted with THF (0.7 mL) was slowly added dropwise for 1 h. The reaction was stirred at −8 °C for 3 h and then cooled to −15 °C. A mixture of K_2CO_3 (2.46 g, 18 mmol), H_2O (10 mL), Et_2NH (2.4 mL) and acetonitrile (10 mL) was added slowly. This solution was stirred for 15 min and then the solvent was removed by rotary evaporation. A saturated aqueous solution of NaCl was added and this solution was extracted with Et_2O. The organic layer was dried over $MgSO_4$ and evaporated. Compound **5** was obtained as a red oil (1.32 g, 95%).

^{1}H NMR (300 MHz, $CDCl_3$): δ = 7.12 (s, 1H), 6.96 (s, 1H), 3.97 (m, 4H), 3.77 (q, 4H), 1.76 (m, 4H), 1.26 (m, 42H), 0.88 (m, 6H). ^{13}C NMR (300 MHz, $CDCl_3$): δ = 150.50, 147.36, 120.80, 111.78, 108.03, 103.73, 71.30, 69.98, 32.07, 29.79, 29.51, 26.17, 22.84, 14.27. EI-MS: $M^{+\bullet}$: 625.55 (18%), 545.55 (7%), 444.50 (100%), 276.30 (54%).

2,5-Bis(dodecyloxy)-4-(2′-trimethylsilylethynyl)-(3′,3′-diethyltriazeno)benzene 6. A solution of compound **5** (1.5 g, 2.4 mmol) in Et_3N (20 mL) was degassed with argon in a sealed tube. Then $PdCl_2$ (42 mg; 0.24 mmol), PPh_3 (94 mg, 0.36 mmol) and $Cu(OAc)_2$ (24 mg, 0.12 mmol) were added. The solution was further degassed and trimethylsilylacetylene (0.86 mL, 6 mmol) was finally added. The reaction mixture was heated at 100 °C for 18 h. The solution was filtered, the precipitate was washed with ethyl acetate and the filtrate was rotary evaporated. The residue was dissolved with ethyl acetate and was washed with a saturated aqueous solution of NaCl, dried over $MgSO_4$ and evaporated. The crude product was purified by flash chromatography (SiO_2, petroleum ether–Et_2O–Et_3N 98 : 1 : 1) to give **6** as a yellow oil (954 mg, 62%).

^{1}H NMR (300 MHz, $CDCl_3$): δ = 6.99 (s, 1H), 6.90 (s, 1H), 3.97 (m, 4H), 3.78 (q, 4H), 1.77 (m, 4H), 1.25 (m, 42H), 0.88 (m, 6H), 0.24 (s, 9H). ^{13}C NMR (300 MHz, $CDCl_3$): δ = 155.73, 146.62, 142.77, 120.58, 109.31, 102.55, 102.23, 97.86, 70.94, 69.36, 32.05, 29.78, 29.61, 29.49, 29.19, 26.22, 22.82, 14.24, 11.74, 0.24. EI-MS: $M^{+\bullet}$: 641.65 (19%), 542.55 (10%), 373.25 (38%), 73.10 (100%).

2,5-Bis(dodecyloxy)-4-(2′-trimethylsilylethynyl)iodobenzene 8. Compound **6** (954 mg, 1.49 mmol) and CH_3I (12.5 mL) were introduced into a sealed tube. The mixture was heated at 120 °C for 18 h. Then the solvent was removed by rotary evaporation. The crude product was purified by flash chromatography (SiO_2, petroleum ether–Et_2O 95 : 5) and 88 mg of **8** as a yellow solid were obtained (yield = 88%).

^{1}H NMR (300 MHz, $CDCl_3$): δ = 7.25 (s, 1H), 6.83 (s, 1H), 3.93 (t, J = 6.6 Hz, 4H), 1.78 (m, 4H), 1.26 (m, 36H), 0.88 (m, 6H), 0.25 (s, 9H). ^{13}C NMR (300 MHz, $CDCl_3$): δ = 154.89, 151.69, 123.79, 116.26, 113.39, 100.82, 99.44, 87.94, 70.09, 69.77, 31.98, 29.70, 29.42, 29.22, 26.06, 22.76, 14.19, 0.00. EI-MS: $M^{+\bullet}$: 668.45 (41%), 543.50 (8%), 404.15 (40%), 331.95 (68%), 316.95 (72%), 235.95 (100%). Mp: 34 °C.

4-{[2′-(2″,5″-Bis(dodecyloxy)-4″-(2′-trimethylsilylethynyl)phenyl)]ethynyl}-2,5-bis(dodecyloxy)-(3′,3′-diethyltriazeno)benzene 9. In a sealed tube, a solution of compound **8** (714 mg, 1.1 mmol) and compound **7** (912 mg; 1.6 mmol) in Et_3N (15 mL) and THF (10 mL) was degassed with argon. Then $PdCl_2$ (10 mg, 0.053 mmol), PPh_3 (42 mg, 0.16 mmol) and $Cu(OAc)_2$ (11 mg; 0.053 mmol) were added. The solution was further degassed before closing the sealed tube. The reaction was heated at 50 °C for 18 h. The solvent was evaporated by rotary evaporation. The crude product was purified by flash chromatography (Al_2O_3; petroleum ether–Et_3N 99 : 1 and then petroleum ether–dichloromethane–Et_3N 69 : 30 : 1) to give **9** as a yellow oil (529 mg, 44%).

^{1}H NMR (300 MHz, $CDCl_3$): δ = 7.07 (s, 1H), 6.95 (s, 1H), 6.94 (s, 1H), 6.92 (s, 1H), 4.01 (m, 8H), 3.79 (q, J = 7.2 Hz, 4H), 1.81 (m, 8H), 1.26 (m, 78H), 0.88 (m, 12H), 0.26 (s, 9H). ES^+-MS: m/z: calcd for $C_{71}H_{124}N_3O_4Si$ 1110.9361; found 1110.9382 $[M + H]^+$.

4-{[2′-(2″-5″-Bis(dodecyloxy)-4″-(2′-trimethylsilylethynyl)phenyl)]ethynyl}-2,5-bis(dodecyloxy)iodobenzene 10. Compound **9** (529 mg, 0.48 mmol) and CH_3I (7.4 mL) were introduced into a sealed tube. The mixture was heated at 120 °C for 18 h. Then the solvent was removed by rotary evaporation. The crude product was purified by flash chromatography (SiO_2, petroleum ether–Et_2O 95 : 5). Compound **10** was obtained as a yellow solid (500 mg, 91%).

^{1}H NMR (300 MHz, $CDCl_3$): δ = 7.29 (s, 1H), 6.94 (s, 1H), 6.93 (s, 1H), 6.89 (s, 1H), 3.96 (m, 8H), 1.81 (m, 8H), 1.26 (m, 72H), 0.88 (m, 12H), 0.26 (s, 9H). ^{13}C NMR (300 MHz, $CDCl_3$): δ = 154.34, 154.18, 153.21, 151.84, 124.05, 117.90, 116.41, 116.07, 114.25, 113.96, 103.00, 96.48, 90.86, 87.49, 70.01, 69.82, 69.21, 31.95, 29.69, 29.39, 26.24, 26.12, 25.99, 22.72, 18.73, 14.15, 0.00. ES^+-MS: m/z: calcd. for $C_{67}H_{113}O_4I$-NaSi 1159.7351; found 1159.7341 $[M + Na]^+$. Mp: 54 °C.

4-{[2′-(2″,5″-Bis(dodecyloxy)-4″-(2′-trimethylsilylethynyl)phenyl)]ethynyl}benzaldehyde 12. A solution of compound **8** (300 mg, 0.45 mmol) and compound **11** (170 mg, 1.3 mmol) in 15 mL of dry Et_3N and 10 mL of dry THF in a sealed tube under argon was degassed. Then $PdCl_2$ (8 mg, 0.045 mmol), PPh_3 (18 mg, 0.067 mmol) and $Cu(OAc)_2$ (4.5 mg, 0.022 mmol) were added. The solution was degassed before closing the sealed tube. The reaction was heated at 50 °C for 18 h. Then the solvents were removed by rotary evaporation. The crude product was purified by flash chromatography (SiO_2; petroleum ether–Et_2O 98 : 2) and 220 mg of **12** as a yellow oil were obtained (yield = 73%).

^{1}H NMR (300 MHz, $CDCl_3$): δ = 10.01 (s, 1H), 7.85 (d, J = 8.1 Hz, 2H), 7.65 (d, J = 8.1 Hz, 2H), 6.97 (s, 1H), 6.95 (s, 1H), 4.01 (m, 4H), 1.81 (m, 4H), 1.26 (m, 36H), 0.88 (m, 6H); 0.27 (s, 9H). ^{13}C NMR (300 MHz, $CDCl_3$): δ = 191.40, 154.18, 153.80, 135.40, 132.05, 129.84, 129.61, 117.18, 116.91, 114.68, 113.27, 101.00, 100.72, 93.91, 90.22, 69.56, 31.98, 29.71, 29.42, 26.11,

22.75, 14.18, 0.00. ES$^+$-MS: m/z: calcd for $C_{44}H_{66}O_3NaSi$ 693.4679; found 693.4675 $[M + Na]^+$.

4-[(4-{[2′-(2″,5″-Bis(dodecyloxy)-4″-(2′-trimethylsilylethynyl)phenyl]ethynyl}-2,5-bis(dodecyloxy)phenyl)ethynyl]benzaldehyde 13. A solution of compound **10** (500 mg, 0.44 mmol) and compound **11** (172 mg, 1.3 mmol) in 15 mL of dry Et_3N and 10 mL of dry THF in a sealed tube under argon was degassed. Then $PdCl_2$ (8 mg, 0.045 mmol), PPh_3 (18 mg, 0.067 mmol) and $Cu(OAc)_2$ (4.5 mg, 0.022 mmol) were added. The solution was degassed before closing the sealed tube. The reaction was heated at 50 °C for 18 hours. Then the solvent was removed by rotary evaporation. The crude product was purified by flash chromatography (SiO_2, petroleum ether–Et_2O 95 : 5) and 443 mg of **13** as a yellow solid were obtained (yield = 88%).

^{1}H NMR (300 MHz, $CDCl_3$): δ = 10.02 (s, 1H), 7.86 (d, J = 8.4 Hz, 2H), 7.66 (d, J = 8.4 Hz, 2H), 7.01 (s, 2H), 6.96 (s, 1H), 6.94 (s, 1H), 4.01 (m, 8H), 1.85 (m, 8H), 1.24 (m, 72H), 0.88 (m, 12H), 0.26 (s, 9H). ^{13}C NMR (300 MHz, $CDCl_3$): δ = 191.91, 154.77, 154.51, 154.03, 153.97, 135.91, 132.57, 130.40, 130.13, 118.04, 117.76, 117.61, 117.52, 115.85, 114.98, 114.47, 113.56, 101.75, 100.76, 94.46, 91.88, 91.12, 90.93, 70.27, 70.06, 32.50, 30.25, 29.94, 26.67, 23.26, 14.68, 2.22. ES$^+$-MS: m/z: calcd for $C_{76}H_{118}O_5NaSi$ 1161.8646; found 1161.8624 $[M + Na]^+$. Mp: 52 °C.

2,5-Bis(dodecyloxy)-(2′-trimethylsilylethynyl)benzene 21. Compound **2** (1.5 g, 2.9 mmol) was dissolved in 15 mL of dry Et_3N and 5 mL of dry THF in a sealed tube under argon. The solution was degassed, then $PdCl_2$ (50 mg, 0.29 mmol), PPh_3 (112 mg, 0.43 mmol) and $Cu(OAc)_2$ (29 mg, 0.14 mmol) were added. The solution was degassed again and the trimethylsilylacetylene (1.01 mL, 7.1 mmol) was added before closing the sealed tube. The reaction was heated at 100 °C for 18 h. The solution was filtered with ethyl acetate and evaporated. The residue was dissolved in ethyl acetate and washed with a saturated aqueous solution of NaCl, dried over $MgSO_4$ and evaporated. The crude product was purified by flash chromatography (SiO_2, petroleum ether–Et_2O 99 : 1) and 1.23 g of **21** as a yellow solid were obtained (yield = 78%).

^{1}H NMR (300 MHz, $CDCl_3$): δ = 6.92 (d, J = 2.7 Hz, 1H), 6.79 (d, J = 2.7 Hz, 1H), 6.77 (s, 1H), 3.94 (t, J = 6.5 Hz, 2H), 3.86 (t, J = 6.5 Hz, 2H), 1.75 (m, 4H), 1.25 (m, 36H), 0.88 (m, 6H), 0.25 (s, 9H). ^{13}C NMR (300 MHz, $CDCl_3$): δ = 154.62, 152.62, 118.56, 116.94, 113.96, 113.29, 101.37, 98.15, 31.91, 29.63, 29.35, 26.01, 22.68, 14.12, 0.00. EI-MS: M^+: 542.60 (69%), 374.35 (33%), 206.20 (76%), 191.20 (100%). Mp: 35 °C.

2-[2′,5′-Bis(dodecyloxy)-4′-(2″-(trimethylsilyl)ethynyl)phenyl]ethynylbenzene 24. A solution of compound **8** (90 mg, 0.13 mmol) and phenylacetylene **23** (0.044 mL, 0.4 mmol) in 3.8 mL of dry Et_3N and 2.6 mL of dry THF in a sealed tube under argon was degassed. Then $PdCl_2$ (2.3 mg, 0.013 mmol), PPh_3 (5.3 mg, 0.02 mmol) and $Cu(OAc)_2$ (1.3 mg, 0.0067 mmol) were added. The solution was degassed before closing the sealed tube. The reaction was heated at 50 °C for 18 h. Then the solvent was evaporated by rotary evaporation. The crude product was purified by flash chromatography (SiO_2, petroleum ether–dichloromethane 90 : 10) and 63 mg of **24** as a yellow oil were obtained (yield = 73%).

^{1}H NMR (300 MHz, $CDCl_3$): δ = 7.51 (m, 2H), 7.33 (m, 3H), 6.96 (s, 1H), 6.94 (s, 1H), 3.99 (m, 4H), 1.81 (m, 4H), 1.25 (m, 36H), 0.88 (m, 6H), 0.26 (s, 9H). ^{13}C NMR (300 MHz, $CDCl_3$): δ = 154.22, 153.52, 131.59, 128.30, 123.48, 118.45, 117.37, 116.94, 114.34, 113.73, 101.20, 100.04, 94.88, 85.92, 69.65, 69.54, 31.94, 29.67, 29.38, 26.08, 22.71, 14.13, 0.04. ES$^+$-MS: m/z: calcd for $C_{43}H_{66}O_2NaSi$ 665.4730; found 665.4725 $[M + Na]^+$. Mp: 31 °C.

[4-{2-[2′,5′-Bis(dodecyloxy)-4′-(2″-(trimethylsilyl)ethynyl)phenyl]ethynyl}-2,5-bis(dodecyloxy)phenyl]ethynylbenzene 25. A solution of compound **10** (70 mg, 0.057 mmol) and phenylacetylene **23** (0.019 mL, 0.17 mmol) in 1.6 mL of dry Et_3N and 1.1 mL of dry THF in a sealed tube under argon was degassed. Then $PdCl_2$ (1 mg, 0.0057 mmol), PPh_3 (2.2 mg, 0.0086 mmol) and $Cu(OAc)_2$ (0.05 mg, 0.0029 mmol) were added. The solution was degassed before closing the sealed tube. The reaction was heated at 50 °C for 18 h. Then the solvent was evaporated by rotary evaporation. The crude product was purified by flash chromatography (SiO_2, petroleum ether–dichloromethane 90 : 10) and 53 mg of **25** as a yellow solid were obtained (yield = 78%).

^{1}H NMR (300 MHz, $CDCl_3$): δ = 7.52 (m, 2H), 7.34 (m, 3H), 7.00 (s, 2H), 6.94 (s, 1H), 6.93 (s, 1H), 3.99 (m, 4H), 1.81 (m, 4H), 1.26 (m, 36H), 1.14 (s, 21H), 0.88 (m, 6H). ^{13}C NMR (300 MHz, $CDCl_3$): δ = 154.70, 153.51, 154.49, 154.48, 131.62, 131.57, 129.30, 128,55, 123.48, 118.56, 117.45, 116.94, 115.26, 114.34, 113.73, 112.30, 101.22, 100.14, 99.18, 99.02, 94.88, 85.86, 69.15, 69.12, 31.63, 29.87, 29.58, 26.27, 22.66, 14.05, 0.00. ES$^+$-MS: m/z: calcd for $C_{81}H_{131}O_4Si$ 1195.9817; found 1195.9812 $[M + H]^+$. Mp: 53 °C.

General procedure for Prato reaction. A mixture of the appropriate aldehyde (0.15 mmol), *N*-methylglycine (132 mg, 1.5 mmol) and fullerene (215 mg, 0.3 mmol) in dry toluene (250 mL) was stirred at reflux for 18 h under argon atmosphere. The solvent was removed by rotary evaporation. The crude product was purified by flash chromatography (SiO_2, from petroleum ether–toluene 7 : 3 to pure toluene) to give a brown solid.

Compound 15. The procedure described above was applied using aldehyde **14** to give **15** (110 mg, 77%).

^{1}H NMR (300 MHz, $CDCl_3$): δ = 7.54 (d, J = 8.4 Hz, 2H), 7.17 (d, J = 8.4, 2H), 4.98 (d, J = 9.6 Hz, 1H), 4.92 (s, 1H), 4.26 (d, J = 9.6 Hz, 1H), 2.79 (s, 3H), 0.23 (s, 9H). ES$^+$-MS: m/z: calcd for $C_{74}H_{20}NSi$ 950.1365; found 950.1354 $[M + H]^+$. Mp >200 °C.

Compound 16. The procedure described above was applied using aldehyde **12** to give **16** (131 mg, 62%).

^{1}H NMR (300 MHz, $CDCl_3$): δ = 7.79 (m, 2H), 7.59 (d, J = 8.1 Hz, 2H), 6.92 (s, 2H), 4.99 (d, J = 9.3 Hz, 1H), 4.95 (s, 1H), 4.27 (d, J = 9.3 Hz, 1H), 3.96 (m, 4H), 2.82 (s, 3H), 1.80 (m, 4H), 1.25 (m, 36H), 0.88 (m, 6H), 0.25 (s, 9H). ES$^+$-MS: m/z: calcd for $C_{106}H_{72}NO_2Si$ 1418.5332; found 1418.5344 $[M + H]^+$. Mp >200 °C.

Compound 17. The procedure described above was applied using aldehyde **13** to give **17** (223 mg, 76%).

^{1}H NMR (300 MHz, $CDCl_3$): δ = 7.80 (m, 2H), 7.60 (d, J = 8.40 Hz, 2H), 6.98 (s, 1H), 6.97 (s, 1H), 6.95 (s, 1H), 6.93 (s, 1H), 4.99 (d, J = 9.30 Hz, 1H), 4.95 (s, 1H), 4.27 (d, J = 9.30 Hz, 1H), 3.97 (m, 8H), 2.82 (s, 3H), 1.81 (m, 8H), 1.26 (m, 72H), 0.88 (m, 12H), 0.26 (s, 9H). ES$^+$-MS: m/z: calcd for $C_{138}H_{124}NO_4Si$ 1886.9300; found 1886.9331 $[M + H]^+$. Mp >200 °C.

Compound 29. $(bpy)_2RuCl_2 \cdot 2H_2O$ (200 mg, 0.38 mmol) and 5-bromo-2,2′-bipyridine **28** (100 mg, 0.42 mmol) were dissolved in a mixture of water (32 mL) and ethanol (16 mL). The solution was stirred at reflux for 3 h under argon atmosphere. The solvents were removed by rotary evaporation. The product was dissolved in a minimum of methanol and was precipitated by addition of a saturated aqueous solution of KPF_6 (25 mL). The orange solid **29** was collected by filtration, washed with water and dried under vacuum (340 mg, 94%).

^{1}H NMR (300 MHz, $CDCl_3$): $\delta = 8.50$ (m, 5H), 8.39 (d, $J =$ 8.7 Hz, 1H), 8.23 (dd, $J = 2.1$ Hz, $J = 8.7$ Hz, 1H), 8.06 (m, 5H), 7.80 (d, $J = 5.4$ Hz, 1H), 7.75 (d, $J = 2.1$Hz, 1H), 7.72 (m, 4H), 7.41 (m, 5H). Mp >200 °C.

General procedure for the cleavage of the TMS protecting group. The appropriate protected acetylenic derivative (1.4 mmol) was dissolved in dichloromethane (20 mL). K_2CO_3 (1.93 mg, 14 mmol) and methanol (40 mL) were added. The solution was stirred at room temperature for 2 h under argon. Water was added and the mixture was extracted with dichloromethane. The organic layer was dried over $MgSO_4$ and evaporated to dryness leading to the free acetylenic derivative sufficiently pure to be used in the next step as such.

2,5-Bis(dodecyloxy)-4-ethynyl-(3′,3′-diethyltriazeno)benzene 7. The procedure described above was applied using **6**. Compound **7** was obtained as a yellow oil (quantitative).

^{1}H NMR (300 MHz, $CDCl_3$): $\delta = 6.95$ (s, 1H), 6.86 (s, 1H), 3.96 (t, $J = 6.6$ Hz, 2H), 3.91 (t, $J = 6.6$ Hz, 2H), 3.72 (q, $J =$ 6.9 Hz, 4H), 3.23 (s, 1H), 1.76 (m, 4H), 1.26 (m, 42H), 0.88 (m, 6H). EI-MS: M^+: 569.65 (26%), 470.55 (4%), 301.35 (25%), 133.15 (12%), 43.25 (100%).

4-Ethynylbenzaldehyde 11. The procedure described above was applied using **14**. **11** was obtained as a white solid (93%).

^{1}H NMR (300 MHz, $CDCl_3$): $\delta = 10.02$ (s, 1H), 7.85 (d, $J =$ 8.1 Hz, 2H), 7.64 (d, $J = 8.1$ Hz, 2H), 3.29 (s, 1H).

Compound 18. The procedure described above was applied using **15** (100 mg, 0.1 mmol), but the reaction was conducted in the following mixture of solvents dichloromethane–toluene–methanol (4 mL : 2 mL : 7.5 mL) and was heated to reflux for 48 h. Compound **18** was obtained as a brown solid (107 mg, 98%).

^{1}H NMR (300 MHz, $CDCl_3$): $\delta = 7.77$ (m, 2H), 7.56 (d, $J =$ 8.1 Hz, 2H), 4.99 (d, $J = 9.6$ Hz, 1H), 4.94 (s, 1H), 4.27 (d, $J =$ 9.6 Hz, 1H), 3.09 (s, 1H), 2.80 (s, 3H).

Compound 19. The procedure described above was applied using **16** (110 mg, 0.077 mmol), but the reaction was conducted in the following mixture of solvents dichloromethane–toluene–methanol (4 mL : 2 mL : 8 mL) and was heated to reflux for 24 h. **19** was obtained as a brown solid (quantitative).

^{1}H NMR (300 MHz, $CDCl_3$): $\delta = 7.80$ (m, 2H), 7.59 (d, $J =$ 7.9 Hz, 2H), 6.96 (s, 2H), 4.99 (d, $J = 9.1$ Hz, 1H), 4.95 (s, 1H), 4.28 (d, $J = 9.1$ Hz, 1H), 3.97 (m, 4H), 3.33 (s, 1H), 2.82 (s, 3H), 1.81 (m, 4H), 1.25 (m, 36H), 0.88 (m, 6H).

Compound 20. The procedure described above was applied using **17** (110 mg, 0.058 mmol), but the reaction was conducted in the following mixture of solvents dichloromethane–toluene–methanol (4 mL : 2 mL : 3 mL) and was heated to reflux for 24 h. **20** was obtained as a brown solid (106 mg, 82%).

^{1}H NMR (300 MHz, $CDCl_3$): $\delta = 7.80$ (m, 2H), 7.60 (d, $J =$ 8.40 Hz, 2H), 6.99 (s, 1H), 6.98 (s, 1H), 6.97 (s, 1H), 6.96 (s, 1H), 5.00 (d, $J = 9.60$ Hz, 1H), 4.95 (s, 1H), 4.27 (d, $J = 9.60$ Hz, 1H), 3.96 (m, 8H), 3.33 (s, 1H), 2.82 (s, 3H), 1.80 (m, 8H), 1.25 (m, 72H), 0.88 (m, 12H).

2,5-Bis(dodecyloxy)ethynylbenzene 22. The procedure described above was applied using **21** and **22** was obtained as a yellow solid (quantitative).

^{1}H NMR (300 MHz, $CDCl_3$): $\delta = 6.97$ (d, J=2.7 Hz, 1H), 6.82 (d, $J = 2.7$ Hz, 1H), 6.79 (s, 1H), 3.97 (t, $J = 6.6$ Hz, 2H), 3.87 (t, $J = 6.6$ Hz, 2H), 3.23 (s, 1H), 1.77 (m, 4H), 1.26 (m, 36H), 0.88 (m, 6H). EI-MS: M^+: 470.45 (22%), 302.35 (24%), 134.20 (100%).

2-[2′,5′-Bis(dodecyloxy)-4′-ethynylphenyl]ethynylbenzene 26. The procedure described above was applied using **24** and **26** was obtained as a yellow oil (quantitative).

^{1}H NMR (300 MHz, $CDCl_3$): $\delta = 7.53$ (m, 2H), 7.49 (m, 3H), 7.00 (s, 1H), 6.98 (s, 1H), 4.00 (m, 4H), 3.34 (s, 1H), 1.82 (m, 4H), 1.27 (m, 36H), 0.89 (m, 6H).

4-{2-[2′,5′-Bis(dodecyloxy)-4′-ethynylphenyl]ethynyl}-2,5-bis(dodecyloxy)phenylethynylbenzene 27. The procedure described above was applied using **25** and **27** was obtained as a yellow-brown solid (quantitative).

^{1}H NMR (300 MHz, $CDCl_3$): $\delta = 7.52$ (m, 2H), 7.34 (m, 3H), 7.01 (s, 1H), 7.00 (s, 1H), 6.98 (s, 1H), 6.97 (s, 1H), 3.99 (m, 4H), 3.34 (s, 1H), 1.81 (m, 4H), 1.26 (m, 36H), 0.88 (m, 6H).

General procedure for Sonogashira cross-coupling with metallo-synthon 29. A solution of compound **29** (50 mg, 0.053 mmol) and the appropriate spacer (1.5 eq., 0.080 mmol) in Et_3N (0.6 mL) and DMF (4 mL) were introduced into a sealed tube and degassed under argon. Then $Pd(dppf)Cl_2$ (8 mg, 0.01 mmol) and CuI (2 mg, 0.01 mmol) were added. The solution was further degassed before closing the sealed tube by pump–freeze cycles. The reaction mixture was heated then water (50 mL) was added and the solution was extracted with dichloromethane. The organic layer was then washed with water, dried over $MgSO_4$ and rotary evaporated. The crude product was first purified by flash chromatography on silica gel and then by size exclusion chromatography (Sephadex LH-20) eluted with THF.

Complex R_1. The procedure described above was applied using spacer **22** and heating at 30 °C for 3 h. Flash column chromatography on SiO_2 using a solvent gradient from pure CH_3CN to CH_3CN–H_2O–aqueous saturated KNO_3 80 : 20 : 5 drops. $\mathbf{R_1}$ was obtained as a red solid (82%).

^{1}H NMR (300 MHz, CD_3OD): $\delta = 8.68$ (m, 6H), 8.11 (m, 6H), 7.85 (m, 6H), 7.51 (m, 5H), 6.92 (s, 2H), 3.96 (t, $J = 6.6$ Hz, 2H), 3.94 (t, $J = 6.6$ Hz, 2H), 1.78 (m, 4H), 1.25 (m, 36H), 0.88 (m, 6H). ES^+-MS: m/z: calcd for $C_{62}H_{76}N_6O_2Ru$ 519.2537; found 519.2547 C^{2+}. Mp: 127 °C.

Complex R_2. The procedure described above was applied using spacer **26** and heating at 45 °C for 18 h. Flash column chromatography on SiO_2 using a solvent gradient from pure dichloromethane to dichloromethane–acetonitrile 80–20. $\mathbf{R_2}$ was obtained as a red solid (45%).

^{1}H NMR (300 MHz, $CDCl_3$): $\delta = 8.43$ (m, 6H), 7.97 (m,6H), 7.70 (m, 6H), 7.48 (m, 7H), 7.33 (m, 3H), 6.97 (s, 1H), 6.96 (s, 1H), 3.94 (m, 4H), 1.74 (m, 4H), 1.25 (m, 36H), 0.88 (m, 6H). ES^+-MS: m/z: calcd for $C_{70}H_{80}N_6O_2Ru$ 569.2693; found 569.2712 C^{++}. Mp: 126 °C.

Complex R_3. The procedure described above was applied using spacer **27** and heating at 45 °C for 18 h. Flash column chromatography on SiO_2 using a solvent gradient from pure dichloromethane to dichloromethane–acetonitrile 80 : 20. $\mathbf{R_3}$ was obtained as a red solid (35%).

^{1}H NMR (300 MHz, $CDCl_3$): $\delta = 8.45$ (m, 6H), 8.01 (m, 6H), 7.72 (m, 6H), 7.44 (m, 7H), 7.35 (m, 3H), 7.02 (s, 1H), 6.99 (s, 1H), 6.98 (s, 2H), 3.99 (m, 8H), 1.79 (m, 8H), 1.24 (m, 72H), 0.86 (m, 12H). ES^+-MS: m/z: calcd. for $C_{102}H_{132}N_6O_4Ru$ 803.4677; found 803.4682 C^{++}. Mp: 120 °C.

Dyad D_1. The procedure described above was applied using spacer **18** and heating at 90 °C for 18 h. Flash column chromatography on SiO_2 using a solvent gradient from pure THF to THF–saturated KPF_6 in methanol 90 : 10. **D_1** was obtained as a red solid (24%).

^{1}H NMR (300 MHz, $CDCl_3$): δ = 8.46 (m, 6H), 8.05 (m, 6H), 7.63 (m, 6H), 7.45 (m, 5H), 7.30 (d, J = 9 Hz, 2H), 6.82 (d, J = 9 Hz, 2H), 3.95 (m, 2H), 3.26 (s, 1H), 2.97 (s, 3H). ES^+-MS: m/z: calcd. for $C_{101}H_{33}N_7Ru$ 722.5920; found 722.5936 C^{++}. Mp >200 °C.

Dyad D_2. The procedure described above was applied using spacer **19** and heating at 90 °C for 18 h. Flash column chromatography on SiO_2 using a solvent gradient from pure THF to THF–saturated KPF_6 in methanol 90 : 10. **D_2** was obtained as a red solid (30%).

^{1}H NMR (300 MHz, $CDCl_3$): δ = 8.39 (m, 6H), 7.99 (m, 6H), 7.68 (m, 8H), 7.58 (d, J = 8.4 Hz, 2H), 7.48 (m, 5H), 6.97 (s, 1H), 6.94 (s, 1H), 4.99 (d, J = 9.0 Hz, 1H), 4.95 (s, 1H), 4.27 (d, J = 9.0 Hz, 1H), 3.94 (m, 4H), 2.82 (s, 3H), 1.85 (m, 4H), 1.25 (m, 36H), 0.88 (m, 6H). ES^+-MS: m/z: calcd for $C_{133}H_{85}N_7O_2Ru$ 956.7904; found 956.7923 C^{++}. Mp >200 °C.

Dyad D_3. The procedure described above was applied using spacer **20** and heating at 30 °C for 18 h. Flash column chromatography on SiO_2 using a solvent gradient from pure THF to THF–saturated KPF_6 in methanol 90 : 10. **D_3** was obtained as a red solid (32%).

^{1}H NMR (400 MHz, $CDCl_3$): δ = 8.47 (m, 6H), 8.04 (m, 6H), 7.79 (m, 8H), 7.61 (d, J = 8.20 Hz, 2H), 7.53 (m, 5H), 6.99 (s, 1H), 6.81 (s, 1H), 6.57 (s, 1H), 5.52 (s, 1H), 5.03 (d, J = 9.55 Hz, 1H), 5.00 (s, 1H), 4.27 (d, J = 9.55 Hz, 1H), 3.97 (m, 8H), 2.83 (s, 3H), 1.87 (m, 8H), 1.25 (m, 72H), 0.88 (m, 12H). MALDI-TOF-MS: m/z: calcd for $C_{165}H_{137}N_7O_4Ru$ 2383.0; found 2382.8. Mp >200 °C.

Results

Synthesis of the compounds

In the study, the alkoxy substituents on the spacers have been introduced only for solubility purposes. However, it is known that electron donating substituents, such as alkoxy groups, increase the π-electron conjugation and decrease the HOMO–LUMO gap in oligo(phenylethynylene) systems.[4] The strategy adopted here for the synthesis of the dyads **D_1–D_3** relies on a convergent modular approach in which the three units, namely the ruthenium trisbipyridine complex, the spacer and the fullerene units, are joined to one another by successive cross-coupling reactions. Recently, there have been considerable efforts in the synthesis of monodisperse phenylethynylene oligomers and several strategies were reported towards this goal.[11,20,21] We adopted a similar methodology to that described by Tour and coworkers, which is a divergent/convergent strategy based on the use of the diethyltriazene functional group.[22] The major advantage of the triazene group comes from its high polarity which makes it possible to cleanly separate by column chromatography the Glaser by-product, which is systematically formed during this type of Sonogashira cross-coupling reaction, from the desired Sonogashira product.[23] The Glaser by-product contains two triazene groups against only one in the Sonogashira product which results in a large difference in the mobility of these two compounds on column chromatography. The other advantage of triazene is its straightforward transformation into an iodo group in high yield by simply heating with methyl iodide.[24]

The preparation of the spacer **10**, required for this work, is shown on Scheme 2. The commercially available bromohydroquinone **1** is etherified with *n*-bromododecane according to a Williamson reaction in 62% yield. Nitration of **2** carried out in a mixture of acetic acid and chloroform afforded the nitro derivative in quantitative yield. The nitro group was reduced with tin in hydrochloric acid and the subsequent diazotization with *tert*-butyl nitrite and boron trifluoride etherate gave the triazene derivative **5** in almost quantitative yield.[25] It is noteworthy that triazene **5** was not purified at this stage, because the crude product was particularly clean and we observed a significant drop in the yield after column chromatography, which was ascribed to the decomposition of triazene on the acidic silica medium. In the next step, the bromo monomer **5** was coupled with trimethylsilylacetylene using the catalytic mixture: $PdCl_2$, $P(Ph)_3$ and $Cu(OAc)_2$. One part of the resulting coupled material **6** was reacted with methyl iodide to transform the triazene into iodide **8** with a 65% yield after purification. The other part was subjected to potassium carbonate to cleave the trimethylsilyl-protecting group of acetylene and gave **7**. Molecules **7** and **8** were then coupled by Sonogashira cross-coupling reaction with the same catalytic conditions as for **6** and resulted in the formation of dimer **9** in 85% yield. Heating **9** in methyl iodide afforded **10** in 80% yield. Finally, iodoarenes **8** and **10** were coupled to the aldehyde **11** to form the precursor for the Prato reaction (Scheme 3).

The attachment of fullerene to the spacers **12–14** was achieved through a 1,3-dipolar cycloaddition reaction of fullerene with azomethine ylide, resulting from the *in situ* reaction of aldehyde with *N*-methylglycine.[26] The deprotection of the trimethylacetylene with potassium carbonate was performed at room temperature and afforded compounds **18–20** in almost quantitative yield. It is important to mention here that the utilization of a triisopropylsilyl group instead of trimethylsilyl for the protection of the ethynyl group in compounds **15–17** did not allow us to obtain **18–20** by desilylation with tetrabutylammonium fluoride. The treatment of the triisopropylsilylacetylene derivatives of **15–17** with tetrabutylammonium fluoride induced a total decomposition of the materials within few minutes probably due to the nucleophilic attack of fluoride anion on the pyrrolidino moiety. The spacers lacking the C_{60} unit, naming **22**, **26** and **27**, for the reference compounds, were synthesized with a similar procedure, but using **23** instead of **11** (Scheme 4).

The preparation of the ruthenium trisbipyridine synthon **29** was obtained by the classical method for preparing ruthenium complexes, which consists in reacting the bromo bipyridine **28** with *bis*bipyridine dichloro ruthenium complex followed by anion metathesis (Scheme 5).[27]

Cross-coupling Sonogashira reactions are less developed with metallo-synthon substrates than with purely organic halides. However, Tor and coworkers[28] have shown that this type of coupling proceeds in good yield using the catalytic mixture $Pd(dppf)Cl_2$ and CuI in DMF (dppf = diphenylphosphinoferrocene). More recently Ziessel and coworkers[10,29,30] reported direct coupling of acetylenic derivatives on polypyridine ruthenium complexes, but using classical Sonogashira conditions. These conditions applied to complex **29** and the spacers **22**, **26–27** or **18–20** led to the expected coupled products with yields varying from 24 to 84%. It is noteworthy that other conditions gave much lower yields for this transformation ($Pd(PPh)_3$–CuI or Fu conditions[31] gave respectively 50% and 0% yields for the formation of **R_1** from **22** and **29**). This shows the importance of the ligand diphenylphosphinoferrocene for the success of this coupling.

Electronic absorption spectra

The spectroscopic absorption data of the dyads **D_1–D_3** and the reference complexes **R_1–R_3** are collected in Table 1 and the spectra of the dyads are shown respectively in Fig. 1 and 2.

The spectra of the reference ruthenium complexes **R_1–R_3** exhibit the absorption bands of the two chromophoric units,

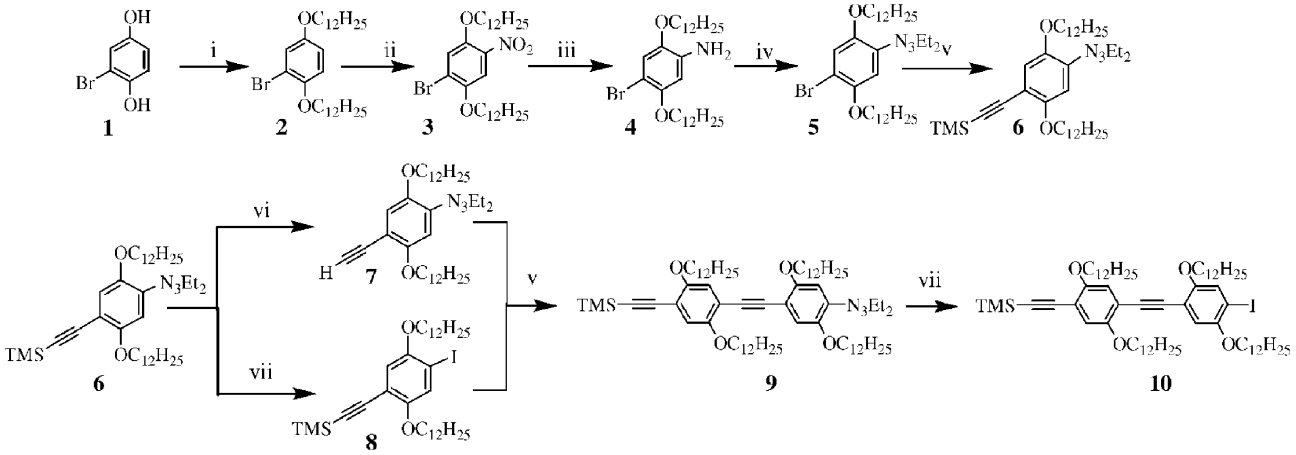

Scheme 2 Synthesis of the spacer **10**. *Reagents and conditions*: i, NaOH, 1-bromododecane in DMF at reflux (62%); ii, acetic acid, HNO_3 in chloroform at rt (97%); iii, tin powder, HCl in THF at rt (92%); iv, $BF_3 \cdot Et_2O$, $tBuNO_2$, in THF at −10 °C (65%); v, trimethylsilylacetylene, $PdCl_2$, PPh_3, $Cu(OAc)_2$ in Et_3N at 100 °C (62%); vi, K_2CO_3, methanol, dichloromethane at rt (100%); vii, CH_3I at 120 °C (88%).

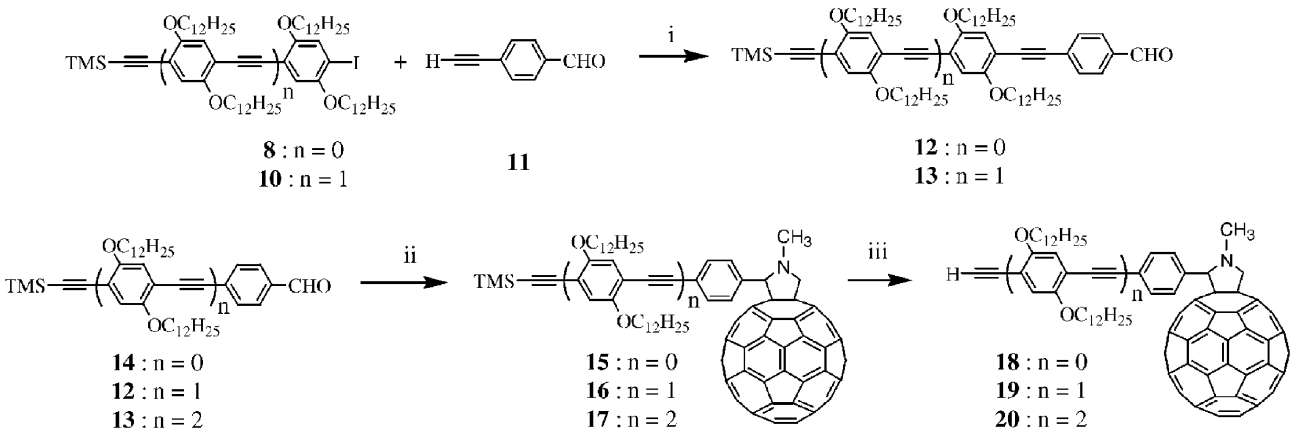

Scheme 3 Synthetic route for the preparation of the spacers **18–20**. *Reagents and conditions*: i, $PdCl_2$, PPh_3, $Cu(OAc)_2$ in Et_3N and THF at 50 °C (73%); ii, *N*-methylglycine and fullerene in dry toluene at reflux (62 to 77%); iii, K_2CO_3, methanol, dichloromethane, toluene at reflux (82 to 100%).

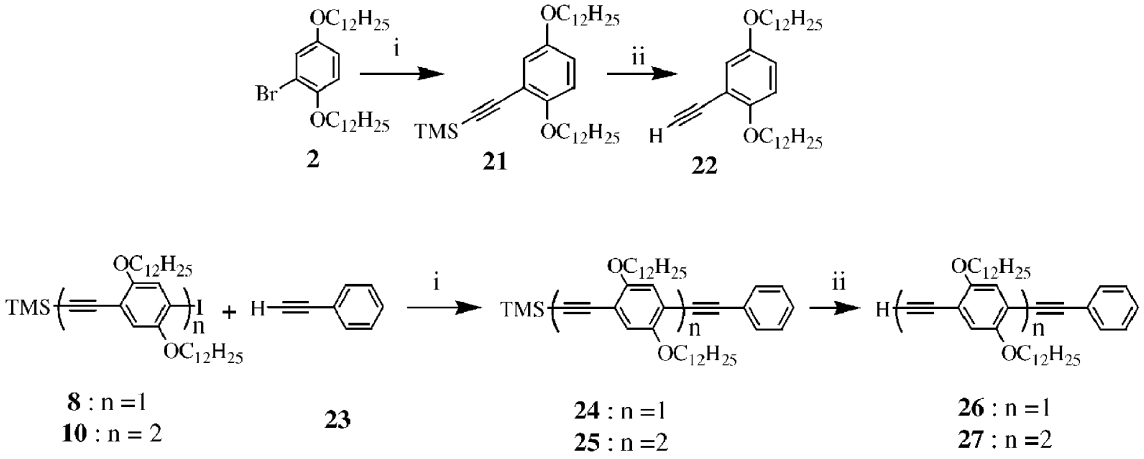

Scheme 4 Synthetic route for the preparation of spacers **22**, **26** and **27**. *Reagents and conditions*: i, trimethylsilylacetylene, $PdCl_2$, PPh_3, $Cu(OAc)_2$ in Et_3N and THF at 100 °C (73 to 78%); ii, K_2CO_3, methanol, dichloromethane at rt (100%).

namely the ruthenium trisbipyridine complex and the oligo (phenylethynylene) spacer. In the UV region, the band at 290 nm is a π–π* transition mostly localized on the bipyridine ligands, whereas the band around 310 nm and which is growing in intensity as the spacer length increases is most certainly attributed to π–π* transitions of the oligo(phenylethynylene) chromophore.

In the visible range, we can see at approximately 450 nm the well-known MLCT transition of the ruthenium complex.[32] In the 350–430 nm region, there is a broad absorption which is

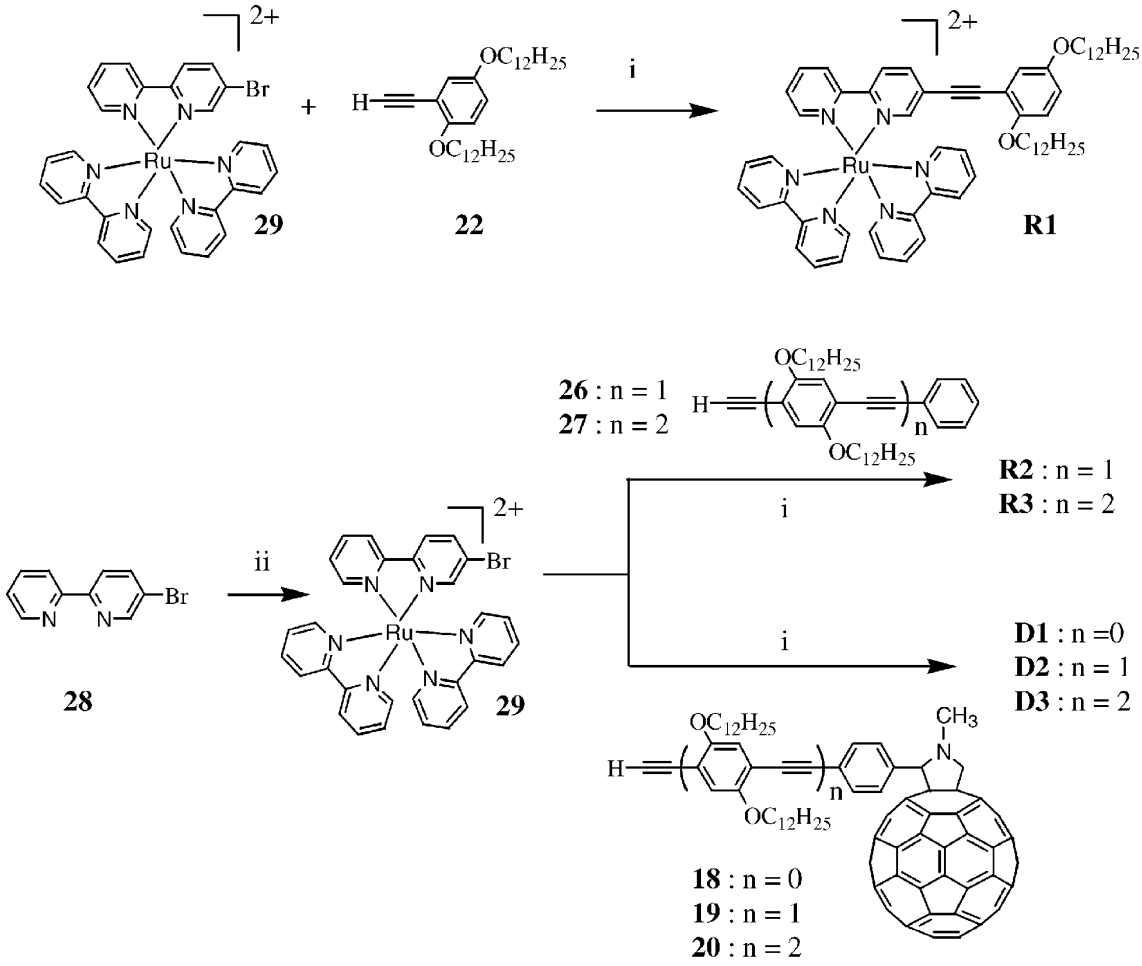

Scheme 5 Preparation of the reference complexes $\mathbf{R_1}$–$\mathbf{R_3}$ and the dyads $\mathbf{D_1}$–$\mathbf{D_3}$. *Reagents and conditions*: i, $Pd(dppf)Cl_2$, CuI in Et_3N and DMF at 30, 45 or 90 °C (24 to 82%).

characteristic of the conjugated oligo(phenylethynylene) spacer.[21] In agreement with other studied examples of this type of molecule, this band is shifted to longer wavelength with a concomitant rise of the molar absorption coefficient as the π-electron system expands.[21,22] This transition is assigned as π–π* transition which is essentially parallel to the long molecular axis of the spacer. Although the π–π* transition of the spacer overlaps significantly with the MLCT transition, this latter band seems to be slightly bathochromically shifted upon attachment of the spacer to the 5 position of the bipyridine (Fig. 2). This indicates that the ground state electronic interactions of the ruthenium complex with the spacer are not very strong, but noticeable. Klemm and coworkers observed that the conjugation length was longer in bipyridine substituted in the 4,4′ positions than those substituted at 5,5′.[33]

In the dyads $\mathbf{D_1}$–$\mathbf{D_3}$, the supplementary chromophore is the fullerene unit. Its spectroscopic signature can be distinguished by the enhanced π–π* band around 310 nm in the UV region of the spectra of the dyads $\mathbf{D_1}$–$\mathbf{D_3}$.[34] The characteristic band of fulleropyrrolidine derivatives can be clearly observed in the spectra of dyads $\mathbf{D_1}$ at 430 nm, but this band is not discernible in dyads $\mathbf{D_2}$–$\mathbf{D_3}$ because it is covered by the intense π–π* transitions of the spacer.

Table 1 Absorption characteristic of the molecules recorded at room temperature in DMF

Compounds	λ_{max}/nm (ε/$M^{-1} \times cm^{-1}$)
$\mathbf{R_1}$	450 (11 100); 378 (17 300); 291 (63 800)
$\mathbf{R_2}$	407 (35 400); 310 (52 600); 291 (75 400)
$\mathbf{R_3}$	421 (52 400); 318 (55 400); 291 (81 300)
$\mathbf{D_1}$	452 (7500); 423 (11 700); 286 (59 400)
$\mathbf{D_2}$	405 (42 100); 318 (82 300); 289 (108 000)
$\mathbf{D_3}$	429 (63 300); 312 (88 300); 287 (119 600)

Electrochemical study

The redox potentials of these novel dyads were studied by cyclic voltammetry at room temperature in dichloromethane and the data are collected in Table 2.

The measured redox potentials are in agreement with the results published on molecules containing similar moieties.[6,30] A common feature of these dyads is the quasi-reversibility of all electrochemical processes. In the cathodic region, the first and the second reduction took place on the fullerene at around −0.6 V and −1.06 V. The third process is attributed to the reduction of the bipyridine unit which is connected to the spacer. This process is shifted to lower potential (∼−1.12 V) compared to a regular ruthenium trisbipyridine complex (−1.32 V).[35] This is most probably a consequence of the stabilization of the LUMO orbitals of the bipyridine which is induced by the π-electron delocalization with the conjugated spacer. In the anodic region, the oxidation of the ruthenium complex took place around 1.36 V and is not significantly modified compared to the unsubstituted ruthenium trisbipyridine complex.

Steady state and time resolved luminescence

The steady state emission spectra were recorded in deaerated acetonitrile solution at room temperature and at 77 K. These

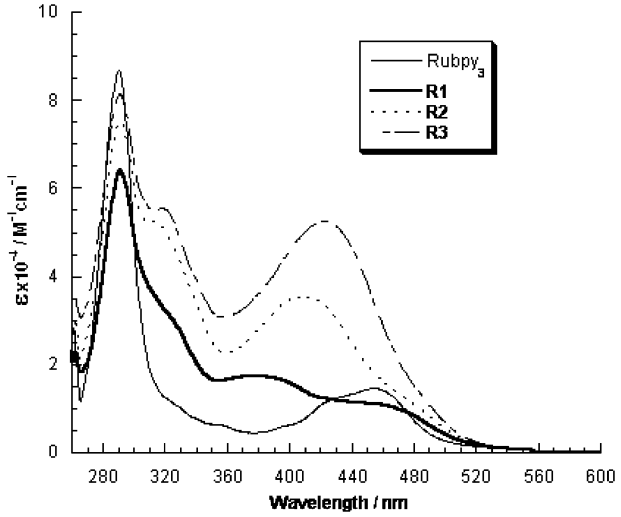

Fig. 1 Overlay of the absorption spectrum of ruthenium trisbipyridine along those of the dyads $\mathbf{R_1}$–$\mathbf{R_3}$ recorded in DMF.

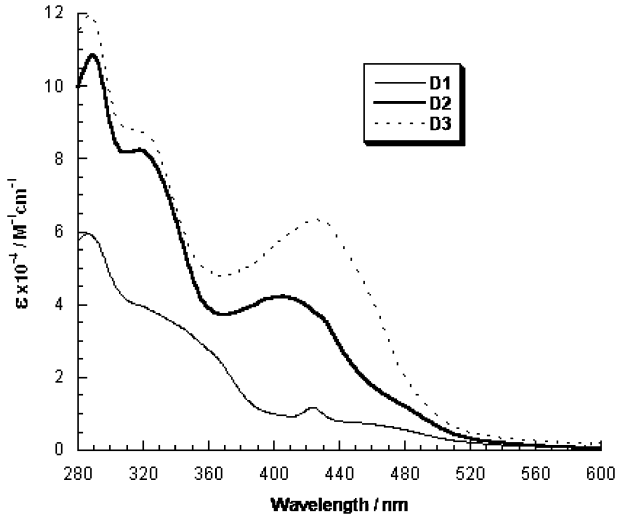

Fig. 2 Overlay of the absorption spectra of dyads $\mathbf{D_1}$–$\mathbf{D_3}$ recorded in DMF.

measurements enabled us to determine both the energy level of the excited state and the percentage of luminescence quenching in dyads $\mathbf{D_1}$–$\mathbf{D_2}$ due to the presence of C_{60}. The pertinent spectroscopic data are collected in Table 3.

The data showed that the emission maximum of the reference complexes $\mathbf{R_1}$–$\mathbf{R_3}$ is shifted to longer wavelength as the spacer length increases (Fig. 3). The bipyridine connected to the spacer is therefore most certainly the ligand where the excited state is localized and this assumption is effective both in the dyad $\mathbf{D_1}$ as well as in the reference $\mathbf{R_1}$. To obtain more details from the 77 K measurements a spectral fit to the data was done using the relation below.[36]

$$I(\bar{\nu}) = \sum_{\upsilon_M}\sum_{\upsilon_L}\left(\frac{\bar{\nu}_{00}-\upsilon_M\bar{\nu}_M-\upsilon_L\bar{\nu}_L}{\bar{\nu}_{00}}\right)^3\left(\frac{S_M^{\upsilon_M}}{\upsilon_M!}\right)\left(\frac{S_L^{\upsilon_L}}{\upsilon_L!}\right)$$
$$\times\left\{\exp\left(-4\ln 2\left(\frac{\bar{\nu}-\bar{\nu}_{00}+\upsilon_M\bar{\nu}_M+\upsilon_L\bar{\nu}_L}{\bar{\nu}_{1/2}}\right)^2\right)\right\}$$

In the expression ν_{00} is the wavenumber of the zero–zero electronic transition, $\bar{\nu}_M$ and $\bar{\nu}_L$ are the wave numbers of vibrational transitions, υ_M and υ_L are vibrational quantum numbers, $\bar{\nu}_{1/2}$ is the full width half maximum (FWHM) of the gaussians and S_M and S_L are the Huang–Rhys factors relating the nuclear distortion between the ground and excited state. In

Table 2 Electrochemical data of the molecules recorded in dichloromethane with 0.15 M Bu_4NPF_6 as supporting electrolyte, potential in V *vs.* SCE. Peak separation were in the range of 60 mV to 100 mV

	Oxidation		Reduction	
Compounds	$E_{Ox}(Ru^{III}/Ru^{II})$/V	$E_{Red}(C_{60}/C_{60}^{-})$/V	$E_{Red}(C_{60}^{-}/C_{60}^{2-})$/V	$E_{Red}(Ru^{II}/Ru^{I})$/V
$Rubpy_3$	1.38			−1.32
$\mathbf{R_1}$	1.35			−1.14
$\mathbf{R_2}$	1.36			−1.13
$\mathbf{R_3}$	1.42			−1.12
$\mathbf{D_1}$	1.39	−0.67	−1.06	−1.17
$\mathbf{D_2}$	1.40	−0.66	−1.02	−1.12
$\mathbf{D_3}$	1.38	−0.63	−1.01	−1.12

the model we assumed, following Meyer and co-workers, that one medium and one low frequency vibrational mode is enough to simulate the experimental data. The wave number for the medium frequency mode was obtained as *ca.* 1450 cm^{-1}, and can be attributed to C–C stretching modes in the ligand. The results presented in Table 4 show that the E_{00} energy, the Huang–Rhys factors and the FWHM of the individual gaussians decrease with increasing length of the phenylethynylene bridge.

The room temperature emission maximum showed a pronounced solvent dependence in $\mathbf{R_1}$. When the polarity of the solvent changed, going from acetonitrile, *via* ethanol, to dichloromethane, the emission maxima changed by almost 20 nm (Table 3). A similar dependence is seen for $[Ru(bpy)_3]^{2+}$ and is expected for the ^{3}MLCT transition. This solvent effect is less pronounced in $\mathbf{R_2}$ and even absent in $\mathbf{R_3}$. This indicates that the nature of the excited state changes as the length of the phenylethylene spacer increase, as will be discussed further below. The idea of a different origin of the excited state was further supported by time resolved emission measurements of $\mathbf{R_1}$–$\mathbf{R_3}$. Thus for $\mathbf{R_1}$: τ = 1.2 μs, for $\mathbf{R_2}$: τ=1.4 μs and for $\mathbf{R_3}$: τ =2.4 μs. The lifetimes of $\mathbf{R_1}$ and $\mathbf{R_2}$ are very similar while the lifetime of $\mathbf{R_3}$ is considerably longer.

The luminescence in dyads $\mathbf{D_1}$–$\mathbf{D_3}$ is almost completely quenched at room temperature, showing only 4% intensity relative to the corresponding reference complex $\mathbf{R_1}$–$\mathbf{R_3}$ (Table 3). The strong quenching of the excited state in $\mathbf{D_1}$–$\mathbf{D_3}$ is confirmed by time-correlated single photon counting measurements in acetonitrile showing a 1000 fold decrease in the lifetime of the luminescence in dyads $\mathbf{D_1}$–$\mathbf{D_3}$ compared to the reference complexes $\mathbf{R_1}$–$\mathbf{R_3}$ (Table 3). Notably the observed lifetime is very similar in $\mathbf{D_1}$–$\mathbf{D_3}$ (τ = 0.6–0.8 ps). The time resolved emission also showed minor components of ~3 ns and ~100 ns contributing to most of the steady-state emission.

Transient spectroscopy study

To follow the fast kinetics of the photo induced processes in $\mathbf{R_1}$–$\mathbf{R_3}$ and $\mathbf{D_1}$–$\mathbf{D_3}$, femtosecond pump–probe experiments were performed on all six molecules in acetonitrile. The molecules were excited with ~100 fs laser pulses at 485 nm, in the red edge of the ruthenium MLCT-band. In $\mathbf{R_1}$–$\mathbf{R_3}$ the transient absorption spectra were constant during the first 5 ns after excitation, except for a $\tau \approx$ 100 ps component, in $\mathbf{R_1}$ and $\mathbf{R_2}$, responsible for a minor absorption rise in the blue part of the spectra contributing to ~10% of the total transient absorption intensity. We tentatively attribute this spectral dynamics to some kind of excited state relaxation.

For $\mathbf{R_1}$, a bleaching of the MLCT ground state band is observed around 480 nm, somewhat overlapping with an excited state absorption band around 440 nm. The latter can be attributed to a LC transition on the substituted bpy that is formally reduced in the MLCT state. In the unsubstituted $[Ru(bpy)_3]^{2+}$ the corresponding band appears around 360

Table 3 Spectroscopic characteristics of compounds studied

Compounds	λ_{em}/nm *RT* ($CH_3CN/EtOH/CH_2Cl_2$)	λ_{em}/nm 77 K (C_3H_7CN)	τ_{em}/ns *RT*	ϕ_{em} (%)[a]	τ_{abs}/ns *RT*
R_1	666/656/648	610, 664	1200	100	0.13
R_2	669/660/658	616, 674	1400	100	0.11
R_3	669/667/669	637, 704	2400	100	[b]
D_1	—	—	0.8	4	0.18, 0.89
D_2	—	—	0.6	4	0.12, 0.57
D_3	—	—	0.8	4	0.17, 0.72

[a] Determined from steady emission spectra and compared to the corresponding reference complex. [b] The amplitude of a possible rise was too small to detect.

nm.[37] In the red part of the spectrum bands are typically attributed to lower transitions of the formally reduced bpy and MLCT from the unreduced ligands to the formally oxidized ruthenium.[38] In **R_2** the excited state absorption bands around 440 and 560 nm are red-shifted to around 480 and 680 nm, consistent with an MLCT state delocalized over a larger bridge. The apparent bleach maximum occurs below 420 nm, which is below the ground state absorption maximum, presumably because of extensive overlap with the excited state absorption. Finally, for **R_3** the apparent ground state bleaching maximizes around 420 nm. The excited state absorption is strong, very broad and relatively featureless, with a weak maximum around 580 nm. This is qualitatively different from **R_1** and **R_2**.

For the complexes **D_1–D_3** the initial spectra formed upon excitation were identical to those of the references (Fig. 4). During the first few nanoseconds these initial excited state spectra changed. The resulting spectra after 4 ns were very similar for the three dyads, with a broad absorption peak around 690 nm (Fig. 4). At the same time the features of the initial, excited state disappeared. The fulleropyrrolidine has a moderate absorption peak around 1010 nm (ε = 8000 M^{-1} cm^{-1})[34,39] and in a separate experiment we tried to detect the $C_{60}^{\bullet -}$ radical by a 1000 nm probe. However, the transient absorption data at this wavelength showed nothing but excited state decay. From these observations we conclude that the new species formed must be the triplet excited state of the fullerene ($^3C_{60}$*) and the resulting spectrum at 4 ns is in good agreement with literature spectra ($\varepsilon \approx$ 10 000 cm^{-1} M^{-1}).[34,39]

The kinetics of the decay of the excited state and build up of $^3C_{60}$* in **D_1–D_3** were followed at 4–5 different wavelengths and a global fit to a sum of exponentials was performed. The analysis of the transient absorption data gave two lifetime components of similar magnitude in all three complexes ($\tau_1 \approx$ 150 ps and $\tau_2 \approx$ 0.6–0.9 ns). For **R_1** and **R_3** a third, smaller component with $\tau_3 \approx$ 5 ns was necessary. We believe that this component originates from excited state dynamics in a subset of complexes with a lower reactivity, possibly an impurity, since the spectral features of this species were very similar to the initially excited spectra. The major component (τ_2) agreed well with the emission lifetimes obtained from the time correlated single photon counting experiments and the global fit gave the following results: for **D_1** (τ = 0.9 ns), for **D_2** (τ = 0.6 ns) and for **D_3** (τ = 0.7 ns). This is attributed to energy transfer to the C_{60} unit. The 150 ps component is instead attributed to excited state dynamics, since this lifetime was observed also in the reference complexes **R_1–R_3**. Indeed, a closer look at the transient absorption spectra of **D_1** around 690 nm where the $^3C_{60}$* absorption peaks clearly shows that the 0.8 ns component gives an increase in the fullerene triplet absorption while the shorter time constant does not (see ESI†).

To follow the slow decay of the formed $^3C_{60}$* we used a flash photolysis setup. In all three complexes **D_1–D_3** the $^3C_{60}$* spectra decayed to the ground state single exponentially with a lifetime, $\tau \approx$ 20 μs and $\lambda_{max} \approx$ 690 nm, which is in good agreement with the reported lifetime and λ_{max} of the fulleropyrrolidine triplet reported by Armaroli[40] (τ = 31 μs, λ_{max} = 690 nm); see Fig. S5.†

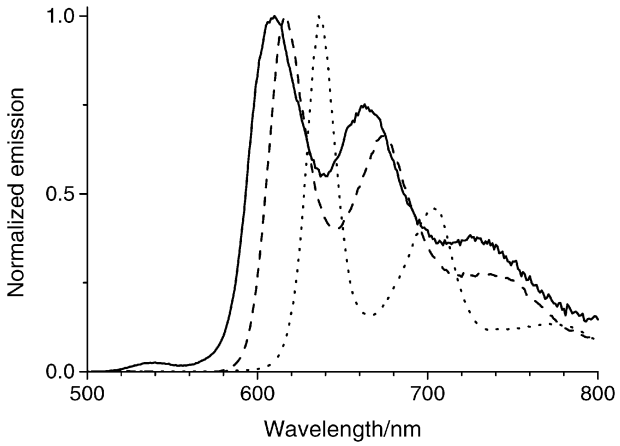

Fig. 3 Overlay of the emission spectrum of the reference complexes **R_1** (solid line), **R_2** (dashed line) and **R_3** (dotted line) recorded at 77 K in butyronitrile.

Discussion

The synthetic molecular approach used to synthesize the dyads **D_1–D_3** relies on the utilization of the performed metallosynthon **29** that was used as a substrate for the Sonogashira cross-coupling reaction. This approach differs from the general strategy that consists in first preparing the bipyridine ligand substituted by the spacer and subsequently performing the coordination chemistry. The synthetic strategy described here could be valuable if the substituent to graft on the bipyridine is either a fragile or a strongly coordinating moiety. In these cases, it can be either damaged or it can compete with the bipyridine ligand during the coordination chemistry step.

According to the redox potentials determined by cyclic voltammetry and the energies of the different excited states calculated from the luminescence study; the strong quenching of the MLCT excited state in dyads **D_1–D_3** could be rationalized by three possible mechanisms.

$$^3Ru^*–S–C_{60} \rightarrow Ru^{III}–S–C_{60}- \rightarrow Ru–S–C_{60} \quad (1)$$

$$^3Ru^*–S–C_{60} \rightarrow Ru^{III}–S–C_{60}- \rightarrow Ru–S–^3C_{60}^* \quad (2)$$

$$^3Ru^*–S–C_{60} \rightarrow Ru–S–^3C_{60}^* \quad (3)$$

Table 4 Spectral fit data from the 77 K emission experiments. In the table the Huang–Rhys factors from the low frequency mode is omitted but they follow the same trend

Compounds	E_{00} /cm^{-1}(eV)	ν_m/cm^{-1}	S_M	$\nu_{1/2}$/cm^{-1}
R_1	16 470 (2.04)	1484	0.88	800
R_2	16 190 (2.01)	1466	0.76	750
R_3	15 690 (1.95)	1475	0.66	560

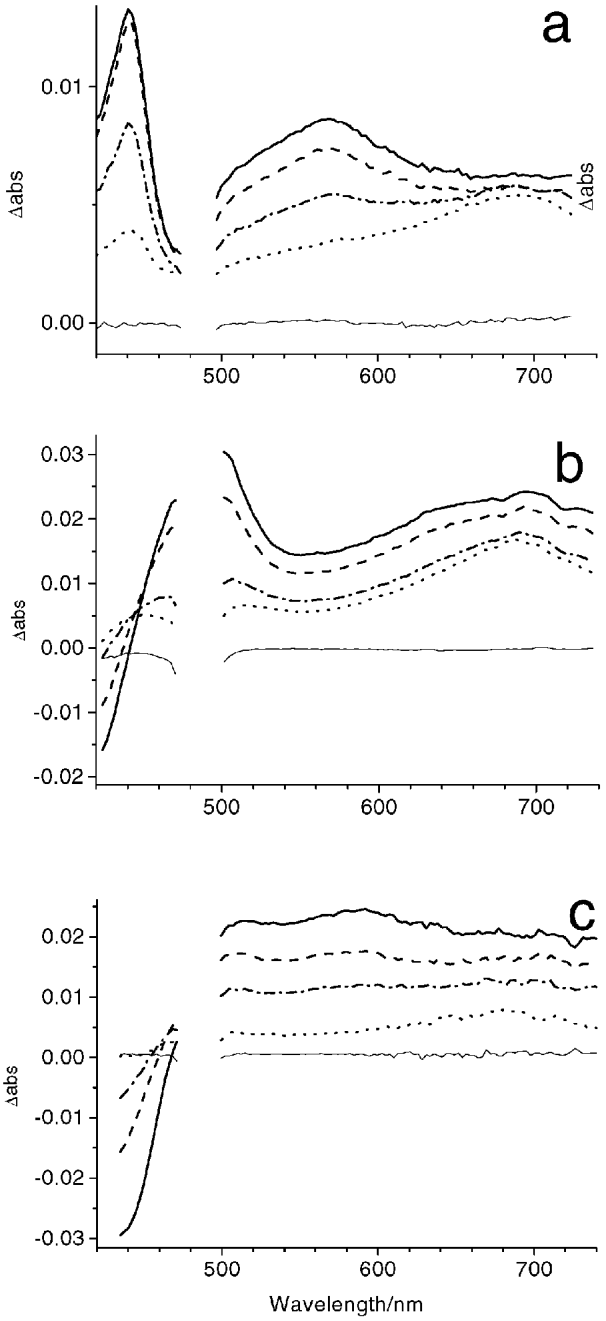

Fig. 4 Transient absorption spectra of $\mathbf{D_1}$ (a), $\mathbf{D_2}$ (b) and $\mathbf{D_3}$ (c) recorded at different times after excitation with a 485 nm laser pulse; 10 ps (solid line), 200 ps (dashed line), 800 ps (dashed-dotted line) and 5 ns (dotted line). The experiments were done in 298 K acetonitrile.

The first is a photoinduced electron transfer that would lead to the intermediate charge separated state composed of the oxidized ruthenium and the reduced fullerene and that would finally recombine to the ground state (eqn (1)). In the second mechanism, the charge separated state can decay to the triplet spin-state of fullerene, since the driving force for this process is substantial ($\Delta G^0_{CS} = -0.31$ eV for dyad $\mathbf{D_2}$ for example) (eqn (2)). The free energy change for charge separation, ΔG^0_{CS} and ΔG^0_{CS}, from the ^{3}Ru* and $^3C_{60}$* respectively, and charge recombination ΔG^0_{CR} can be estimated from the Rehm–Weller equation [41] and based on the electrochemical and luminescence data. ΔG^0_S takes into account the solvation energy due to the solvent change between electrochemistry (CH_2Cl_2, ε_R 9.0) and photochemistry (CH_3CN, $\varepsilon_S = 38.8$). The Coulombic term was omitted because of the large distance between the charges.

$$-\Delta G^0_{CS} = E_{0\text{–}0}(^3C_{60}^*) + \Delta G^0_{CR}$$
$$-\Delta G^0_{CS} = E_{0\text{–}0}(^3Ru^*) + \Delta G^0_{CR}$$
$$-\Delta G^0_{CR} = E^0_{Ru} - E^0_{C_{60}} + \Delta G^0_S$$
$$\Delta G^0_S = (e^2/8\pi\varepsilon_0)[(1/\varepsilon_{AN} - 1/\varepsilon_{DCM})((9\text{–}4)/r_{Ru} + 1/r_{C_{60}})]$$

$E_{0\text{–}0}(^3Ru^*)$, $E_{0\text{–}0}(^3C_{60}^*)$, E^0_{Ru}, $E^0_{C_{60}}$, r_{Ru}, $r_{C_{60}}$ refer, respectively to the energy of the MLCT triplet excited state, the energy of the fullerene triplet excited state (1.45 eV), the $Ru^{3+/2+}$ potential, the $C_{60}^{0/-}$ potential, the radius of ruthenium trisbipyridine (7.0 Å) and the radius of the fullerene (4.4 Å).

A similar mechanism to 2 was indeed reported by Armaroli and coworkers to explain the formation of the triplet excited state of fullerene in ruthenium and rhenium bipyridine complexes connected to a fullerene unit.[7] The third deactivation mechanism is a direct energy transfer leading to the fullerene triplet excited state but without passing through the intermediate charge separated state (eqn (3)). It is important to note that in these dyads, the photoinduced energy transfer process is much more exergonic ($\Delta G_{EnT} = -0.56$ eV for dyad $\mathbf{D_2}$ for example) than the photoinduced charge separation ($\Delta G_{CS} = -0.25$ eV as calculated from the Rehm–Weller equation indicated above for dyad $\mathbf{D_2}$ for example).

$$\Delta G^0_{EnT} = E_{0\text{–}0}(^3Ru^*), - E_{0\text{–}0}(^3C_{60}^*)$$

The transient absorption spectra recorded in acetonitrile did not feature at any time any signal around 1000 nm, which is the well-known specific region diagnostic for the fullerene radical anion fingerprint. The formation of the charge-separated state is therefore ruled out, at least as a long-lived intermediate state. In the light of these observations, we conclude that the formation of an intermediate charge separated state in dyads $\mathbf{D_1}$–$\mathbf{D_3}$ is unlikely, which suggests that mechanisms 1 and 2 are not important in the deactivation of the dyads. Instead energy transfer to the C_{60} unit quenches the MLCT excited state.

For the energy transfer in $\mathbf{D_1}$–$\mathbf{D_3}$ a Förster type dipole–dipole mechanism is excluded due to the negligible spectral overlap between the C_{60}-absorption and the ruthenium-spacer emission.[42] The rate of emission quenching in dyads $\mathbf{D_1}$–$\mathbf{D_3}$ is almost independent of the distance between the ruthenium complex and the fullerene unit (Table 3) and this excludes also a Dexter type energy transfer *via* a simple superexchange type mechanism, since this rate should fall off exponentially with distance as the orbital overlap decreases. The participation of the excited state of the spacer itself in the energy transfer is therefore likely, and the bridge-localized excited state is indeed expected to be close in energy to the ^{3}MLCT state. The role of the spacer could be either to substantially delocalize the ruthenium ^{3}MLCT excited state out on the phenylethylene bridge forming a "super-donor state",[9,43] thus decreasing the effective energy transfer distance. An alternative mechanism is that a triplet state of the spacer itself becomes populated. In other words, the energy is first transferred to the spacer before arriving at the fullerene (eqn (4)).

$$^3Ru^*\text{–}S\text{–}C_{60} \rightarrow Ru\text{–}^3S^*\text{–}C_{60} \rightarrow Ru\text{–}S\text{–}^3C_{60}^* \qquad (4)$$

Assessment of the energy of the triplet excited state of phenyl ethynylene derivatives has been reported by Schanze and coworkers[13,44] and by Köhler and coworkers.[45] From these studies, we estimate that the energy of the spacer triplet excited state is certainly in the range of 1.85–2.1 eV in dyads $\mathbf{D_2}$ and $\mathbf{D_3}$ with the lowest value for $\mathbf{D_3}$. This means that the triplet $\pi \rightarrow \pi^*$ state of the spacer probably becomes populated in $\mathbf{D_3}$ and that the corresponding state is thermally accessible from the ^{3}MLCT excited state of the ruthenium complex in $\mathbf{D_2}$ and possibly also $\mathbf{D_1}$.

The solvent independence of the $\mathbf{R_3}$ emission clearly supports the idea of a stepwise energy transfer since the π–π^* emission from the aromatic spacer should be fairly indepen-

dent of the solvent polarity. It strongly suggests that the lowest excited state of the system is that localized on the spacer. On the other hand, the solvent dependence in $\mathbf{R_1}$ is explained by the charge transfer character of the ruthenium ^{3}MLCT excited state, which should be stabilized by more polar solvents. Also the relatively long emission lifetime in $\mathbf{R_3}$ and the qualitatively different transient absorption spectrum favor a spacer based excited state. Possibly the relatively fast rate of the forbidden deactivation in $\mathbf{R_3}$, and the significant emission, is due to spin–orbit coupling with the heavy ruthenium center.

Further support for the π–π* character of the lowest excited state of $\mathbf{R_3}$ was obtained from the 77 K emission spectra (Fig. 3). The trend of the excited state energy for $\mathbf{R_1}$–$\mathbf{R_3}$ obtained from the spectral fit to the steady-state emission data shows a substantial decrease when going form $\mathbf{R_2}$ to $\mathbf{R_3}$: E_{00} = 2.04, 2.01 and 1.95 eV in the series $\mathbf{R_1}$–$\mathbf{R_3}$. The same trend is seen for the Huang–Rhys factors of the medium frequency mode: S_M = 0.88, 0.76, and 0.66 in the same series. The Huang–Rhys factor and the band-width ($\nu_{1/2}$) for $\mathbf{R_3}$ is extremely low if it were to originate from a ruthenium-to-bipyridine ^{3}MLCT state and reflects a small nuclear displacement when going from the ground to the excited state. This is most probable if the excited state of $\mathbf{R_3}$ is actually the π → π* state of the phenylethylene spacer. Note that the expression for the spectral composition used is based on a general theory for radiative decay and its use is not restricted to MLCT emission. As the medium frequency modes are dominating, these are likely to be similar in frequency for the pyridine and phenyl breathing modes.

In conclusion the π–π* state of the spacer is the lowest excited state of the $\mathbf{R_3}$ chromophore. The initial transient absorption spectrum for $\mathbf{D_3}$ is identical to that for the reference complex $\mathbf{R_3}$. This shows that the excited ruthenium MLCT state rapidly forms the π–π* state of the spacer, which subsequently transfers energy to the C_{60} unit. In $\mathbf{D_1}$ and $\mathbf{D_2}$ the corresponding π–π* state is higher in energy but most likely accessible by thermal population so that energy transfer to the C_{60} unit may be facilitated by a hopping mechanism. Our experiments suggest an interesting alternative for long-range energy transfer where the excited state is efficiently transferred *via* near-isoenergetic bridge states. The intermediate population of the bridge states, which decrease in energy as the spacer length increases, may rationalize the surprisingly constant energy transfer rates over edge-to-edge distances between 1.1 and 2.3 nm for $\mathbf{D_1}$–$\mathbf{D_3}$.

Acknowledgements

The authors acknowledge financial support from the French Ministry of Research with the ACI "jeunes chercheurs" 4057 (salary of FC), the Swedish Foundation for Strategic Research, The Wallenberg Foundation, The Royal Swedish Academy of Sciences, The Swedish Research Council and The Swedish Energy Agency.

References

1 V. Balzani and F. Scandola, *Supramolecular Photochemistry*, Ellis Horwood, Chichester, U.K., 1991.
2 (*a*) M. Bixon and J. Jortner, *Adv. Chem. Phys.*, 1999, **106**, 35; (*b*) S. Encinas, F. Barigelletti, A. M. Barthram, M. D. Ward and S. Campagna, *Chem. Commun.*, 2001, 277; (*c*) S.-I. Kawahara, T. Uchimaru and S. Murata, *Chem. Commun.*, 1999, 563.
3 (*a*) E. A. Weiss, M. J. Ahrens, L. E. Sinks, M. A. Ratner and M. R. Wasielewski, *J. Am. Chem. Soc.*, 2004, **126**, 9510; (*b*) B. P. Paulson, J. R. Miller, W.-X. Gan and G. Closs, *J. Am. Chem. Soc.*, 2005, **127**, 4860; (*c*) W. B. Davis, W. A. Svec, M. A. Ratner and M. R. Wasielewski, *Nature*, 1998, **396**, 60.
4 P. Wautelet, M. Moroni, L. Oswald, J. Le Moigne, A. Pham, J. Y. Bigot and S. Luzzati, *Macromolecules*, 1996, **29**, 446.
5 (*a*) D. Sun, F. S. Tham, C. A. Reed, L. Chaker and P. D. W. Boyd, *J. Am. Chem. Soc.*, 2002, **124**, 6604; (*b*) A. Lutzen, M. Hapke, J. Griep-Raming, D. Haase and W. Saak, *Angew. Chem., Int. Ed.*, 2002, **41**, 2086.
6 N. Martin, L. Sanchez, B. Illescas and I. Perez, *Chem. Rev.*, 1998, **98**, 2527.
7 N. Armaroli, G. Accorsi, D. Felder and J. -F. Nierengarten, *Chem.-Eur. J.*, 2002, **8**, 2314.
8 (*a*) D. Armspach, E. C. Constable, F. Diederich, C. E. Housecroft and J.-F. Nierengarten, *Chem.-Eur. J.*, 1998, **4**, 723; (*b*) M. D. Meijer, G. P. M. van Klink and G. van Koten, *Coord. Chem. Rev.*, 2002, **230**, 141; (*c*) D. M. Guldi, M. Maggini, E. Menna, G. Scorrano, P. Ceroni, M. Marcaccio, F. Paolucci and S. Roffia, *Chem.-Eur. J.*, 2001, **7**, 1597; (*d*) M. Maggini, D. M. Guldi, S. Mondini, G. Scorrano, F. Paolucci, P. Ceroni and S. Roffia, *Chem.-Eur. J.*, 1998, **4**, 1992.
9 N. P. Redmore, I. V. Rubtsov and M. J. Therien, *J. Am. Chem. Soc.*, 2003, **125**, 8769.
10 C. Goze, D. V. Kozlov, F. N. Castellano, J. Suffert and R. Ziessel, *Tetrahedron Lett.*, 2003, **44**, 8713.
11 (*a*) A. Khatyr and R. Ziessel, *J. Org. Chem.*, 2000, **65**, 3126; (*b*) J. M. Tour, *Chem. Rev.*, 1996, **96**, 537; (*c*) J. M. Tour, *Acc. Chem. Res.*, 2000, **33**, 791.
12 (*a*) R. Ziessel, *Synthesis*, 1999, 1839; (*b*) R. E. Martin and F. Diederich, *Angew. Chem., Int. Ed.*, 1999, **38**, 1351; (*c*) Y. Liu, S. Jiang and K. S. Schanze, *Chem. Commun.*, 2003, 650; (*d*) D. Holten, D. F. Bocian and J. S. Lindsey, *Acc. Chem. Res.*, 2002, **35**, 57.
13 K. A. Walters, K. D. Ley, C. S. Cavalaheiro, S. E. Miller, D. Gosztola, M. R. Wasielewski, A. P. Bussandri, H. van Willigen and K. S. Schanze, *J. Am. Chem. Soc.*, 2001, **123**, 8329.
14 P. F. H. Schwab, F. Fleischer and J. Michl, *J. Org. Chem.*, 2002, **67**, 443.
15 I. P. Evans, A. Spencer and G. Wilkinson, *J. Chem. Soc., Dalton Trans.*, 1973, 204.
16 T. Hayashi, M. Konishi, Y. Kobori, M. Kumada, T. Higuchi and K. Hirotsu, *J. Am. Chem. Soc.*, 1984, **106**, 158.
17 L. Hegedus, in *Organometallics in Synthesis. A Manual*, ed. M. Schlosser, John Wiley & Sons, Chichester, 1994, ch. 5, p. 448.
18 O. Johansson, M. Borgstrom, R. Lomoth, M. Palmblad, J. Bergquist, L. Hammarström, L. Sun and B. Åkermark, *Inorg. Chem.*, 2003, **42**, 2908.
19 M. Andersson, J. Davidsson, L. Hammarström, J. Korppi-Tommola and T. Peltola, *J. Phys. Chem. B*, 1999, **103**, 3258.
20 (*a*) J. M. Tour, A. M. Rawlett, M. Kozaki, Y. Yao, R. C. Jagessar, S. M. Dirk, D. W. Price, M. A. Reed, C.-W. Zhou, J. Chen, W. Wang and I. Campbell, *Chem.-Eur. J.*, 2001, **7**, 5118; (*b*) C. A. Briehn and P. Baeuerle, *Chem. Commun.*, 2002, 1015; (*c*) T. Gu, D. Tsamouras, C. Melzer, V. Krasnikov, J.-P. Gisselbrecht, M. Gross, G. Hadziioannou and J.-F. Nierengarten, *Chem. Phys. Chem.*, 2002, **3**, 124; (*d*) T. Gu and J. F. Nierengarten, *Tetrahedron Lett.*, 2001, **42**, 3175; (*e*) J. Zhang, D. J. Pesak, J. L. Ludwick and J. S. Moore, *J. Am. Chem. Soc.*, 1994, **116**, 4227.
21 U. H. F. Bunz, *Chem. Rev.*, 2000, **100**, 1605.
22 J. M. Tour, J. S. Schumm and D. L. Pearson, *Angew. Chem., Int. Ed. Engl.*, 1994, **33**, 1360.
23 P. Siemsen, R. C. Livingston and F. Diederich, *Angew. Chem., Int. Ed.*, 2000, **39**, 2632.
24 D. B. Kimball and M. M. Haley, *Angew. Chem., Int. Ed.*, 2002, **41**, 3338.
25 M. P. Doyle and W. J. Bryker, *J. Org. Chem.*, 1979, **44**, 1572.
26 N. Tagmatarchis and M. Prato, *Synlett*, 2003, 768.
27 D. Hesek, Y. Inoue, S. R. L. Everitt, H. Ishida, M. Kunieda and M. G. B. Drew, *Inorg. Chem.*, 2000, **39**, 308.
28 D. J. Hurley and Y. Tor, *J. Am. Chem. Soc.*, 2002, **124**, 3749.
29 R. Ziessel, V. Grosshenny, M. Hissler and C. Stroh, *Inorg. Chem.*, 2004, **43**, 4262.
30 A. Barbieri, B. Ventura, F. Barigelletti, A. De Nicola, M. Quesada and R. Ziessel, *Inorg. Chem.*, 2004, **43**, 7359.
31 T. Hundertmark, A. F. Littke, S. L. Buchwald and G. C. Fu, *Org. Lett.*, 2000, **2**, 1729.
32 K. Kalyanasundaram, *Photochemistry of Polypyridine and Porphyrin Complexes*, Academic Press, London, 1992.
33 (*a*) U. W. Grummt, T. Pautzsch, E. Birckner, H. Sauerbrey, A. Utterodt, U. Neugebauer and E. Klemm, *J. Phys. Org. Chem.*, 2004, **17**, 199; (*b*) T. Pautzsch and E. Klemm, *Macromolecules*, 2002, **35**, 1569.
34 D. M. Guldi and M. Prato, *Acc. Chem. Res.*, 2000, **33**, 695.
35 (*a*) M. Hissler, A. Harriman, A. Khatyr and R. Ziessel, *Chem.-Eur. J.*, 1999, **5**, 3366; (*b*) K. R. J. Thomas, J. T. Lin, H.-M. Lin, C.-P. Chang and C.-H. Chuen, *Organometallics*, 2001, **20**, 557.
36 (*a*) J. V. Caspar and T. J. Meyer, *Inorg. Chem.*, 1983, **22**, 2444; (*b*) J. A. Treadway, B. Loeb, R. Lopez, P. A. Anderson, F. R. Keene and T. J. Meyer, *Inorg. Chem.*, 1996, **35**, 2242; (*c*) L. Hammarström, F. Barigelletti, L. Flamigni, M. T. Indelli, N. Armaroli,

G. Calogero, M. Guardigli, A. Sour, J.-P. Collin and J.-P. Sauvage, *J. Phys. Chem. A*, 1997, **101**, 9061.
37 A. Yoshimura, M. Z. Hoffman and H. Sun, *J. Photochem. Photobiol., A: Chem.*, 1993, **70**, 29.
38 M. Beley, S. Chodorowski, J.-P. Collin, J.-P. Sauvage, L. Flamigni and F. Barigelletti, *Inorg. Chem.*, 1994, **33**, 2543.
39 D. M. Guldi, H. Hungerbuehler and K.-D. Asmus, *J. Phys. Chem.*, 1995, **99**, 9380.
40 N. Armaroli, F. Barigelletti, P. Ceroni, J.-F. Eckert, J.-F. Nicoud and J.-F. Nierengarten, *Chem. Commun.*, 2000, 599.
41 D. Rehm and A. Weller, *Isr. J. Chem.*, 1970, **8**, 259.
42 (*a*) T. Forster, *Ann. Physik*, 1948, **2**, 55; (*b*) T. Forster, *Energy Commun.*, 1965, **FSU-2690-18**, 61.
43 M. Biswas, P. Nguyen, T. B. Marder and L. R. Khundkar, *J. Phys. Chem. A*, 1997, **101**, 1689.
44 (*a*) K. A. Walters, K. D. Ley and K. S. Schanze, *Chem. Commun.*, 1998, 1115; (*b*) K. D. Ley, C. E. Whittle, M. D. Bartberger and K. S. Schanze, *J. Am. Chem. Soc.*, 1997, **119**, 3423.
45 A. Köhler, J. S. Wilson, R. H. Friend, M. K. Al-Suti, M. S. Khan, A. Gerhard and H. Bassler, *J. Chem. Phys.*, 2002, **116**, 9457.